AD-A052 910 FLORIDA UNIV GAINESVILLE F/G 8/7
STUDY OF FEASIBILITY OF USING WISSA-TYPE PIEZOMETER PROBE TO ID--ETC(U)
FEB 78 J H SCHMERTMANN DACW39-76-M-6646
UNCLASSIFIED WES-TR-S-78-2 NL

1 OF 1
AD
A052910

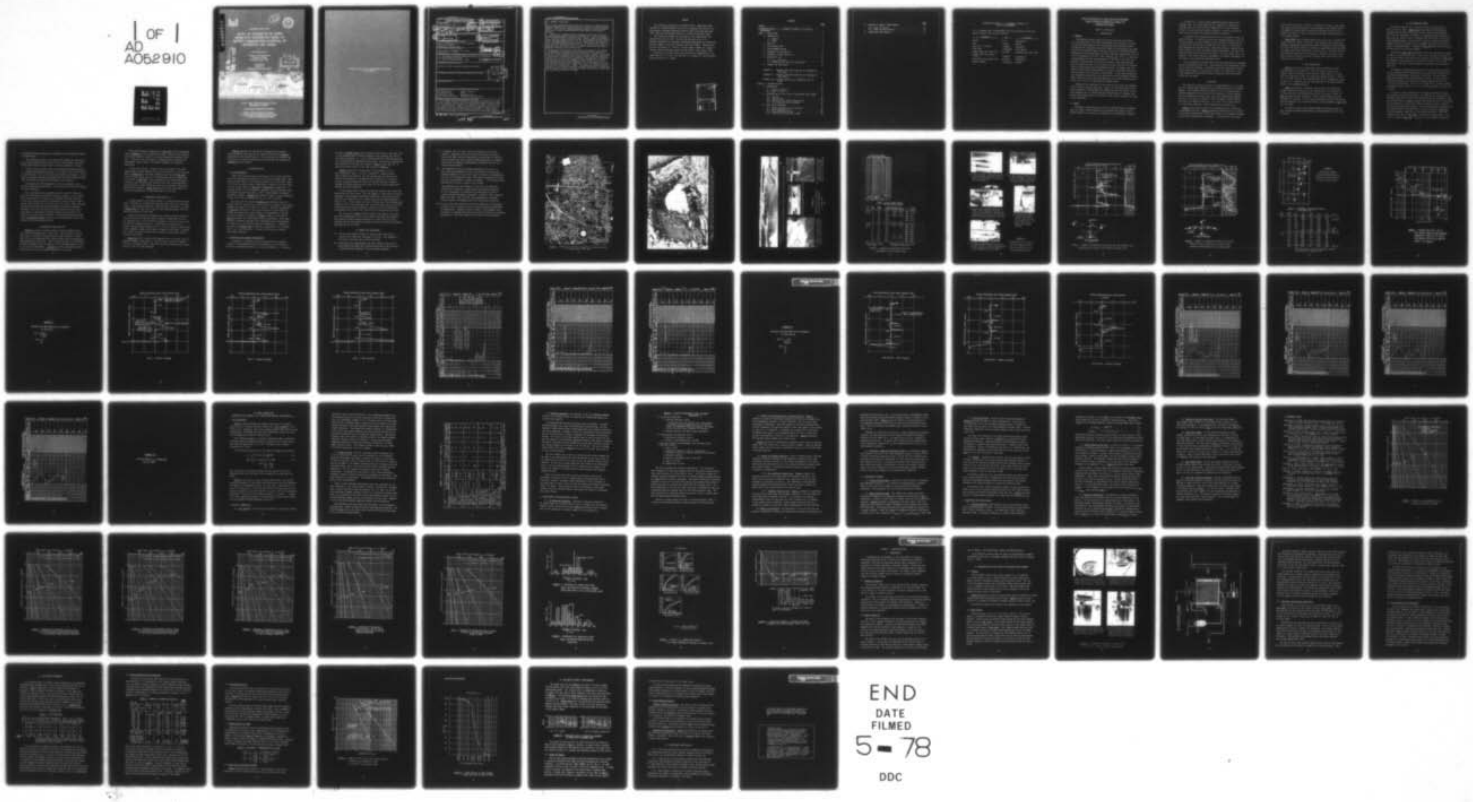

END
DATE
FILMED
5-78
DDC

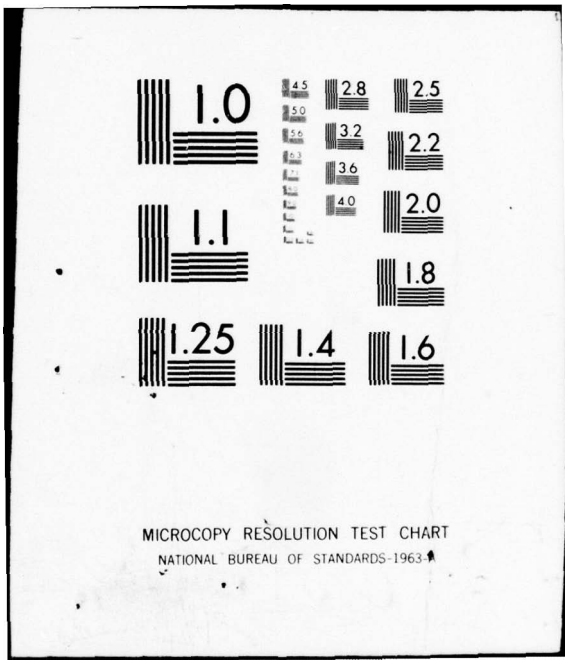
1.0
1.1
1.25
1.4
1.6
1.8
2.0
2.2
2.5
2.8
3.2
3.6
4.0
4.5
5.0
5.6
6.3
MICROCOPY RESOLUTION TEST CHART
NATIONAL BUREAU OF STANDARDS-1963-A

TECHNICAL REPORT S-78-2

STUDY OF FEASIBILITY OF USING WISSA-TYPE PIEZOMETER PROBE TO IDENTIFY LIQUEFACTION POTENTIAL OF SATURATED FINE SANDS

by

John H. Schmertmann

Professor of Civil Engineering
University of Florida
Gainesville, Florida 32611

February 1978
Final Report

Approved For Public Release; Distribution Unlimited

Prepared for Office, Chief of Engineers, U. S. Army
Washington, D. C. 20314

Under Contract No. DACW39-76-M-6646

Monitored by Soils and Pavements Laboratory
U. S. Army Engineer Waterways Experiment Station
P. O. Box 631, Vicksburg, Miss. 39180

Destroy this report when no longer needed. Do not return it to the originator.

Unclassified

SECURITY CLASSIFICATION OF THIS PAGE (When Data Entered)

REPORT DOCUMENTATION PAGE

READ INSTRUCTIONS BEFORE COMPLETING FORM

1. REPORT NUMBER: Technical Report S-78-2	2. GOVT ACCESSION NO.: WES
3. RECIPIENT'S CATALOG NUMBER: TR-S-78-2	
4. TITLE (and Subtitle): STUDY OF FEASIBILITY OF USING WISSA-TYPE PIEZOMETER PROBE TO IDENTIFY LIQUEFACTION POTENTIAL OF SATURATED FINE SANDS	5. TYPE OF REPORT & PERIOD COVERED: Final report
	6. PERFORMING ORG. REPORT NUMBER
7. AUTHOR(s): John H. Schmertmann	8. CONTRACT OR GRANT NUMBER(s): Contract No. DACW39-76-M-6646
9. PERFORMING ORGANIZATION NAME AND ADDRESS: John H. Schmertmann, Ph. D., P.E., Consultant University of Florida Gainesville, Florida 32611	10. PROGRAM ELEMENT, PROJECT, TASK AREA & WORK UNIT NUMBERS
11. CONTROLLING OFFICE NAME AND ADDRESS: Office, Chief of Engineers, U. S. Army Washington, D. C. 20314	12. REPORT DATE: Feb 78 13. NUMBER OF PAGES: 72
14. MONITORING AGENCY NAME & ADDRESS (if different from Controlling Office): U. S. Army Engineer Waterways Experiment Station Soils and Pavements Laboratory P. O. Box 631, Vicksburg, Miss. 39180	15. SECURITY CLASS. (of this report): Unclassified 15a. DECLASSIFICATION/DOWNGRADING SCHEDULE

16. DISTRIBUTION STATEMENT (of this Report)

Approved for public release; distribution unlimited.

DDC RECEIVED APR 19 1978 F

17. DISTRIBUTION STATEMENT (of the abstract entered in Block 20, if different from Report)

18. SUPPLEMENTARY NOTES

19. KEY WORDS (Continue on reverse side if necessary and identify by block number)

Cone penetrometers	Relative density
Fine grained soils	Sands
Liquefaction (soils)	Saturated soils
Pore pressure measurement	Wissa-type piezometer probe

20. ABSTRACT (Continue on reverse side if necessary and identify by block number)

A two-phase study was performed to investigate the feasibility of using the pore pressure response from a penetrating Wissa piezometer probe to indicate the potential for liquefaction in saturated fine sand. The Wissa probe is a cone penetrometer, similar to the Dutch cone penetrometer, with a sensing element at the tip for measurement of pore pressures. Phase I was a field study consisting of three piezometer probe tests to a depth of about four and one-half meters in each of two areas; Area 1 containing deposits of

(Continued) → next Page

DD FORM 1 JAN 73 1473 EDITION OF 1 NOV 65 IS OBSOLETE

Unclassified

SECURITY CLASSIFICATION OF THIS PAGE (When Data Entered)

139 900

20. ABSTRACT (Continued).

loose, easily liquefiable mine tailings sand, and Area 2 containing similar deposits compacted by a vibratory roller to a condition of stable relative density. Tests in Area 1 produced generally positive excess pore pressures, while tests in Area 2 produced generally small negative pore pressure response.

Phase II was a laboratory study consisting of four tests, each on a freshly prepared specimen of Reid-Bedford Model sand, in the 4 ft diameter by 4 ft high University of Florida triaxial chamber. Relative densities in these tests were between 30 and 81 percent, the mid-height vertical effective stress was approximately 17.5 psi, K_o was approximately 0.46, and the degree of saturation approximately 97 percent. The pore pressure response in these tests was qualitatively similar to that in the field tests, but of a magnitude about one-tenth as great. The reduced response was attributed to imperfect saturation of the test specimens.

Comparison of pore pressure data with relative density, as estimated from approximate correlations with penetrometer resistance, suggest that this type of probe sounding can detect very unstable, saturated, clean, fine sands with relative densities below about 20 percent. However, there may be a broad range of relative density in which the piezometer probe response is insensitive to relative density. Additionally, the magnitude of pore pressure generated at the tip of a Wissa-type probe depends not only on the effective stresses and dilatancy behavior of the in situ sand but also on its permeability and the rate of penetration used. This study was done with only one rate of penetration, 2 cm/sec. In applying this method for field estimation of liquefaction potential, associated measurements of permeability will be required. Possibly these can be obtained from the rate of pore pressure decay when penetration is stopped.

PREFACE

This report was prepared by Professor John H. Schmertmann under Contract No. DACW39-76-M-6646 as part of the ongoing work at the U. S. Army Engineer Waterways Experiment Station (WES) under CWIS Work Unit 31144, entitled "Earthquake Resistance of Earth and Rockfill Dams."

The study was initiated at the request of Mr. Ralph Beene, who monitored the work for OCE. The work was directed by Dr. A. G. Franklin, Research Civil Engineer, Earthquake Engineering and Vibrations Division (EE&VD), Soils and Pavements Laboratory (S&PL). General guidance was provided by Dr. Francis G. McLean, Chief, EE&VD, Mr. Stanley J. Johnson, Special Assistant, S&PL, and Mr. James P. Sale, Chief, S&PL.

Directors of the WES during this study and the preparation of the report were COL G. H. Hilt, CE, and COL J. L. Cannon, CE. The Technical Director was Mr. F. R. Brown.

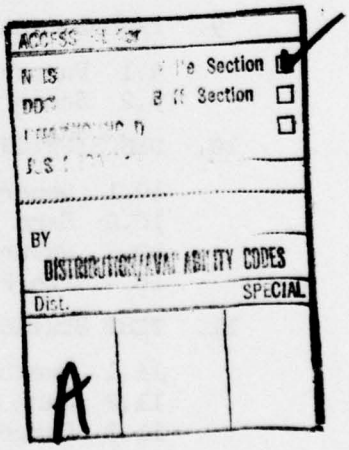

CONTENTS

CONVERSION FACTORS, U. S. CUSTOMARY TO METRIC (SI)
UNITS OF MEASUREMENT

U. S. customary units of measurement used in this report can be converted to metric (SI) units as follows:

Multiply	By	To Obtain
inches	25.4	millimetres
feet	0.3048	metres
miles (U. S. statute)	1.609344	kilometres
cubic feet	0.02831685	cubic metres
pounds (mass) per cubic foot	16.01846	kilograms per cubic metre
pounds (force) per square inch	6.894757	kilopascals
tons (force) per square foot	95.76052	kilopascals
degrees (angle)	0.01745329	radians

STUDY OF FEASIBILITY OF USING WISSA-TYPE PIEZOMETER PROBE TO IDENTIFY LIQUEFACTION POTENTIAL OF SATURATED FINE SANDS

PHASE I - FIELD STUDY

1. INTRODUCTION

1.1 Purpose

This progress report presents the results from the first phase of a two phase study. The study investigates the feasibility of using the pore pressure response from a penetrating Wissa piezometer probe to indicate the liquefaction potential stability of saturated, fine sand. We know from references such as those in the A.S.C.E. 1975 GED Specialty Conference on In Situ Measurement of Soil Properties (Schmertmann, Vol. II, p. 96; Torstensson, Vol. II, p. 48; Wissa et. al., Vol. I, p. 523) that a penetrating probe with the approximate 10 cm^2 area of the Dutch cone produces a pore pressure field around the probe. This field probably has a net positive value in loose sands and weak clays and a net negative value in dense sands and overconsolidated clays. We imagine that such behavior results from either negative or positive dilatency behavior of loose and dense soil structures, respectively. It then seems reasonable that liquefaction potential, also associated with such dilatency behavior, might correlate with the sign and magnitude of the pore pressures generated at the point of a penetrating cone-shaped probe.

Judging by the literature, no one seems to have tried this approach, even in a pilot study of this type. Phase I of the present pilot study had the purpose of investigating the feasibility of this type of in situ pore pressure test to evaluate liquefaction potential of a single, saturated, fine sand deposit in the field. Phase II will continue the study in the laboratory.

1.2 Scope

The Phase I scope includes a total of 6 piezometer probe soundings, each to a depth of about $4\frac{1}{2}$ meters in saturated, fine sands, all performed within two test areas at a single site in Jacksonville, Florida.

One area, No. 1, had an easily liquefied surface layer of mine tailings sand. The second area, No. 2A, consisted of similar mine tailings sand, but which had been compacted with a heavy vibratory roller to a stable relative density condition. We could not make the sand in area 2A exhibit any signs of dynamic instability.

I performed three piezometer probe tests, or soundings, in each of these two areas. In each area we made two soundings using the type of c. 20° point angle, 1.75 inch diameter, probe described by Wissa, et. al. I rented such a probe from Dr. Wissa for this study. At each area I also performed one sounding using a previously purchased, similar probe made by Wissa, but with a tip shape closely matching the cone shape used with the Dutch cone penetration test (CPT) -- 60° point angle and 1.5 in. diameter. This study thus also investigated the relative performance of two shapes of the Wissa-type piezometer probe.

I also performed seven Dutch CPTs in the area immediately surrounding the above piezometer probe tests. This permitted some correlation between the two types of soundings. In addition, previous correlations between static cone bearing, q_c, and relative density, D_r, permitted at least rough estimates of the relative density condition of the sands probed in the two test areas.

2. THE SITE

The study site consists of part of an approximately 0.5 x 1.0 mile area of tailings sand remaining from the mining operations of the DuPont Company. This company removed the upper c. 15 ft of alluvial sand by hydraulic dredge and then extracted the few percent of heavy minerals from an otherwise pure quartz sand. They then hydraulically replaced the bulk of the sand, now washed of fines and almost entirely quartz, back into the original excavations. But, much of this sand returned in a very loose condition. Mining stopped about 20 years ago.

Figure 1 shows the location of the tailings area on a portion of a Jacksonville city map. Figure 2 presents an aerial photo of a portion of the larger tailings area. The portion shown is the currently planned site for the "hidden Lakes" development. It includes the test areas

used in this study, Nos. 1 and 2A, as located in the area. This figure also shows the survey pattern of cone penetration tests (CPTs) used to investigate the larger area to permit the efficient location of the special test areas. I have not included these CPTs (except CPT-15) in this progress report.

Figure 3(a) shows a panorama ground view of the site to permit the reader to get the "feel" of the area. The washing of the sand by the hydraulic pumping and heavy mineral extraction operations removed almost all fines and organic materials, leaving an organically inert sand which can support only little vegetation, or none at all. The result was the large sand dune areas shown in the photos. However, over most of the area, between the dunes, we found the ground water level within one to three feet of the surface.

3. THE TAILINGS SAND

Figure 4 presents an average grain size distribution for the tailings sand at the study site. From the results of many sieve analyses (made by others) the -200 fraction varies from 0.1 to 1.0%, with an average about 0.3%. The underlying natural sand has a -200 of about 2 to 4%. Note the very uniform nature of the tailings sand, with C_u about 1.2. Inspection of this sand indicates it is almost entirely quartz, with subangular grains.

Table 1 (below Fig. 4) presents some in-place and maximum and minimum density information from the tailings sand. We obtained the in-place data from two dewatered test pits in test area 2, shown in Fig. 2, using the sand cone method. The max and min densities were determined at the Univ. of Fla. using the Burmister method ("The importance and practical use of relative density in soil mechanics", Proc. ASTM, Vol. 84, 1948).

In addition, others have performed ASTM D-1557 Proctor tests on this sand and obtained modified Proctor optimum densities of 102.1 and 103.8 pcf.

4. THE PIEZOMETER PROBES

As noted in section 1.2, we used two types of Wissa probes at each of the test sites. Figure 5(a) shows a photo of these probes together with the Dutch mantle cone tip used with the matching CPTs. The top probe, identified as "Wissa", is essentially that described in Wissa, et. al. (1975), with the exception that the bottom of the porous steel sensing element at the point of the cone has a porous horizontal surface instead of the impervious cone-shaped cap shown in the illustration in the Wissa paper. I rented the Fig. 5(a) probe from Dr. Wissa, and he reports it is now his standard.

The probe in Fig. 5(a) identified as "UF" also came from Dr. Wissa. He made it to order for the Univ. of Fla. so as to match as closely as he could the shape of the Dutch cone tip shown at the bottom of Fig. 5(a). We performed one sounding with the UF probe at each of the two test areas (Nos. 1 and 2A), located between the two Wissa probe soundings in each area.

We carefully calibrated each probe for its pore pressure response in the laboratory before taking them out into the field, using the same recording instrumentation as we used in the field. We also checked these calibrations after returning from the field. In all cases the calibration remained the same for both probes, namely 1.0 chart div. = 0.5 psi water pressure. One div. has a width of 0.1 inches, allowing a reading accuracy of about + or - 0.1 psi water pressure, or about 3 in. of water.

We tried to assure saturation of the probe just before actually penetrating the sand with the probe. We assembled the various parts of the probe under water, after first boiling the porous tip element. Then, still under water, we wrapped a plastic bag around the point of the probe, with the bag full of water and a sponge covering the point to protect the bag against premature rupture. We then taped the bag top against the cylindrical sides of the probe above its cone, as shown in Fig. 5(c). After pre-digging a small hole to the ground water level, under the sounding truck shown in Fig. 5(b), we lowered the bagged probe to this level, as shown in Fig. 5(c). This gave us our reference reading for

the hydrostatic water pressure and subsequent excess hydrostatic pressure calculations.

The subsequent advance of the probe then ruptured the bag and the probe entered saturated soil for the rest of the sounding. Our chart record always showed a small "blip" to mark the rupture of the bag.

We also tested the probe after its withdrawal following completion of a sounding by immediately placing it in a pail of water and moving it up and down about 6 in. to check its chart response sensitivity. In all cases it responded properly, suggesting that the probes always retained their saturation and sensitivity throughout each sounding.

Both probes had TYCO transducers with 25 psi capacity, + and -, and with 100% overload protection. At no time did we exceed the capacity of these transducers.

Once a piezometer probe sounding started we kept the time-base chart recorder running continuously during the approx. 2 cm/s constant rate of penetration of the probe, in one-meter rod length intervals. At the end of each such meter of penetration we had a delay of about 2 minutes while placing the next meter rod in the system. Each such waiting period permitted significant dissipation of the pore pressures existing at the end of the previous meter penetration and it took a small amount of additional penetration during the next meter to re-establish the pore pressure condition. The individual probe sounding logs in Appendices I and II note some of these penetration rates, time intervals, and pore pressure effects.

5. SOUNDINGS IN TEST AREA NO. 1

Figure 6 presents the results from the three piezometer probe and three CPT soundings made in this area. Part (a) shows the superposed logs of computed excess hydrostatic water pressure vs. depth. Part (b) has the superposed CPT q_c-depth profiles from the immediately surrounding Dutch cone tests. Part (c) shows the plan of the Wissa and UF probe soundings within the pattern of the surrounding CPTs, as well as the order of performance. Appendix I has the individual logs from both the probe and cone soundings performed in this area.

Note that the probe sounding logs in Fig. 6(a), and the individual logs in Appendix I, do not represent raw data. Instead I have reduced the raw chart data to convert it to excess hydrostatic pressure, both + and -. Note also that both types of soundings used the same rate of penetration, about 2 cm/s, in one meter increments of continuous penetration.

I chose test area No. 1 because it was in an area of very weak tailings sand, as demonstrated by the very low values of q_c in the logs shown in Figure 6(b). Our probe sounding truck, shown in Fig. 5(b), could only move around this site by being pulled with the dozer shown in the photo in Fig. 5(d). After completion of the probe soundings in this area I had the dozer move around the site with a twisting motion and found that it easily worked the sand into an unstable, rolling and almost quick condition. Figure 5(d) shows this dozer sunk about 2 ft after this demonstration of sand instability in this area.

6. SOUNDINGS IN TEST AREA NO. 2A

In sharp contrast to the above area No. 1, area 2A had been treated with 12 coverages of a BROS VP-20D vibratory roller with 10.8 tons dead weight. This treatment produced a stable tailings sand layer. As shown in Figure 5(e) the same dozer using the same twisting motions could not produce instability in this area.

Careful and systematic measurements of tailings surface elevations before and after the vibratory roller compaction showed that the 30' x 30' compaction test area 2A settled an average of 0.90 ft over the $\frac{1}{2}$ that included the sounding study area. Converting this settlement to a relative density change average over the 2 to 14 ft depth of sand affected by the compaction produces an average D_r change of about 45%. I estimate that at this test area we began with an initial D_r about 40%, and thus ended with about 85%.

Figure 3(a) shows a ground level panorama view of the site, with the vehicles working in test area 2A. Parts (b) and (c) show the dramatic effects of vibratory rolling. Part (d) shows the settlement that occurred after 6 of the 12 roller coverages.

Figure 7 presents the same kind of superposed pore pressure probe and CPT data and plan for the stable test area 2A as Figure 6 presented for the unstable area 1. I have included the detailed logs from each of the area 2A piezometer probe and Dutch cone soundings in Appendix II of this report.

7. ANALYSES OF DATA

7.1 q_c-D_r correlation

Other than the gross tests by the dozer, I do not have any direct tests for liquefaction potential of the test area tailings sands. But, such potential relates to the relative density, D_r, of the sand. While I do not have relative density measurements at either of the test areas 1 or 2A, we did obtain the Fig. 6(b) and Fig. 7(b) q_c-depth data. I have previously, for other purposes, prepared a q_c-D_r correlation based on estensive testing in the Univ. of Fla. large diameter, laboratory calibration chamber. Appendix III presents a report on this calibration. I hoped to use this to estimate D_r via q_c at the test areas.

The data base for the above Appendix III calibration does not include effective stress levels as low as those that apply to the surface tailings sand layer at the study test areas. I therefore extrapolated the App. III correlation to the very low effective stress range and checked the predicted D_r values against the measurements we did have of relative density, as reported in Table I herein for test area 2. Figure 8 presents the measured-predicted D_r comparisons. This figure indicates reasonable agreement when considering all the possibilities for error in the lab and field density determinations. I therefore considered the Appendix III correlation as applicable to the tailings sand at the study test areas -- at least in its initial, normally consolidated condition.

7.2 Normalized pore pressure measurements

I attempted to normalize the excess hydrostatic pore pressure response of the piezometer probes by considering such in relation to effective overburden pressures, σ_v', and cone bearing, q_c. I reviewed

the data in Figures 6 and 7 and at various depth levels in each test area I chose average values of excess hydrostatic pore pressure, Δu, and of cone bearing capacity, q_c. I also computed effective overburden pressure, σ_v', and normalized by dividing by this value. In this way I obtained the data detailed in the right hand columns of Table 2 (below Fig. 8). I then plotted these points on the semi-log plot of Figure 9.

Figure 9 presents the final product of this Phase I of this pilot feasibility study. At first I attempted to separate points from the Wissa and UF probes, but then decided that the data did not justify such separation. Considering soil variability, it seemed to me that both probes generated about the same pore pressure responses, although the Wissa probe gave more detail and the UF probe perhaps gave somewhat greater Δu magnitude.

It also appears that a large pore pressure response only occurs when penetrating very loose sands. The data suggests a large range of relative densities, and presumably liquefaction potentials, over which the probe pore pressure response does not produce large pore pressure magnitude, either + or -. In my opinion, at least for sands with their permeabilities similar to that of this tailings sand, this probe method does not provoke a sufficient pore pressure response to provide a tool with sufficient discrimination for useful field exploration for liquefaction potential.

The two points in Fig. 9 from the natural sand suggest that sands with lower permeability, such as silty sands, may produce much greater pore pressure response during penetration at 2 cm/s than the subject tailings sand and thus produce the greater sensitivity needed for adequate discrimination in the field.

8. SUMMARY AND CONCLUSIONS

8.1 - The two pore pressure probes of the Wissa type used in this research both worked well throughout the study. They appeared to give good, consistent data at both test areas.

8.2 - Both probes gave approximately the same response, with the 20° Wissa perhaps providing more layering detail and the 60° UF probe a somewhat greater magnitude of pore pressure generated.

8.3 - It appears that this type of probe sounding can detect very unstable, saturated, clean, fine sands with relative densities below about 20%. However, there may be a broad range of relative density wherein this type of probe sounding does not have adequate sensitivity for adequate descrimination of relative density and liquefaction potential.

8.4 - The magnitude of the pore pressure generated at the tip of a Wissa type probe depends not only on the effective stresses and dilatency behavior of the in situ sand, but also on its permeability and the rate of penetration used. This study investigated with only one rate of penetration. We also do not know the tailings sand's permeability, nor how it varies in the deposit.

When applying this probe method to a new site with relatively unknown soil conditions, a high positive pore pressure response in a fine sand might be interpreted as indicating low relative density and high liquefaction potential. Actually, such a response might come from a silt with much lower permeability and higher relative density, and perhaps also lower liquefaction potential.

8.5 If we use this probe method for the field estimating of liquefaction potential, then I believe we will also need associated measurements of permeability. Perhaps the rate of decay of pore pressure from the moment of stopping penetration could form the basis for estimating permeability. This pilot study did not explore this possibility.

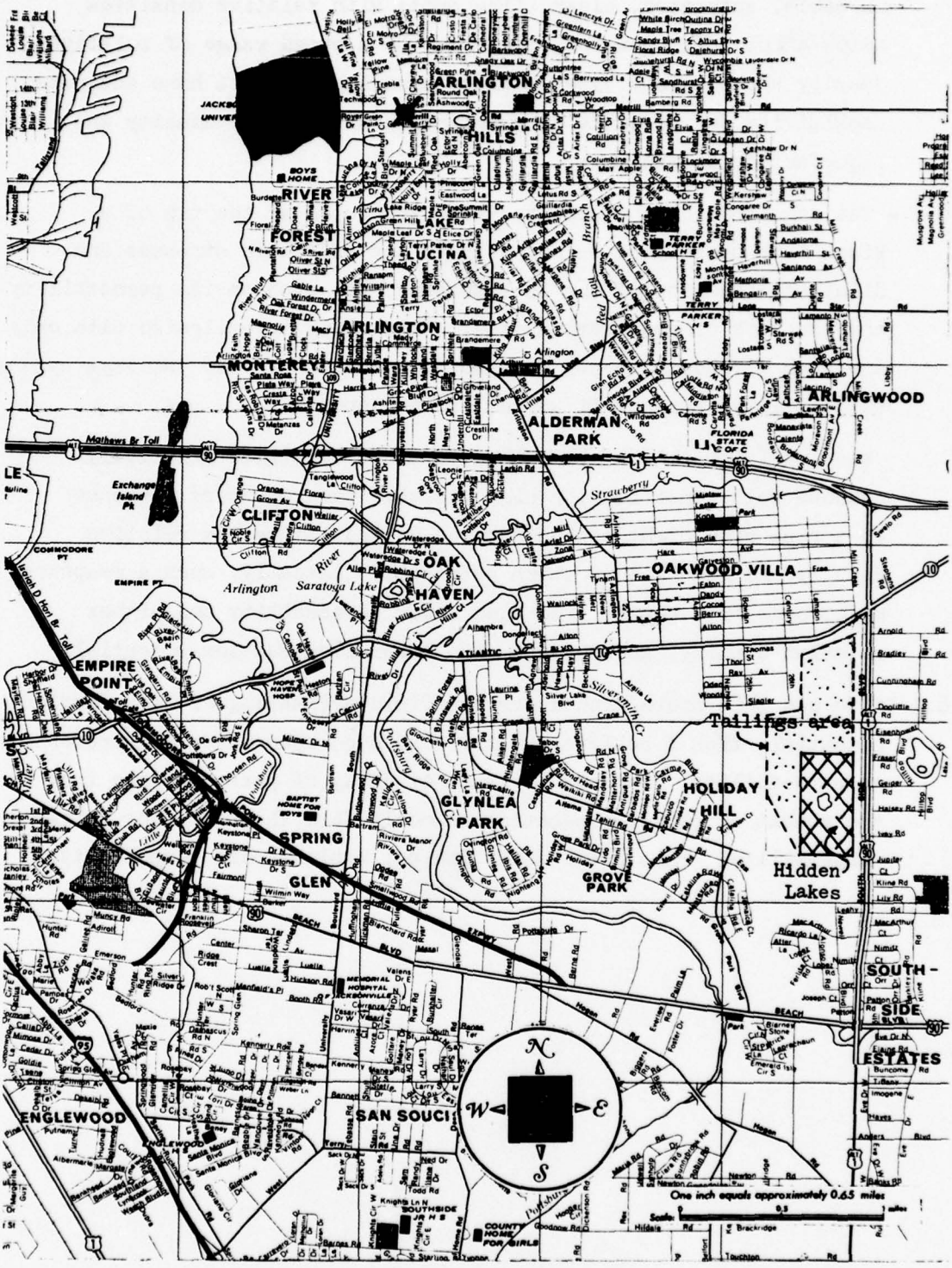

FIGURE 1 - PORTION OF CITY MAP OF JACKSONVILLE SHOWING LOCATION OF "HIDDEN LAKES" STUDY AREA

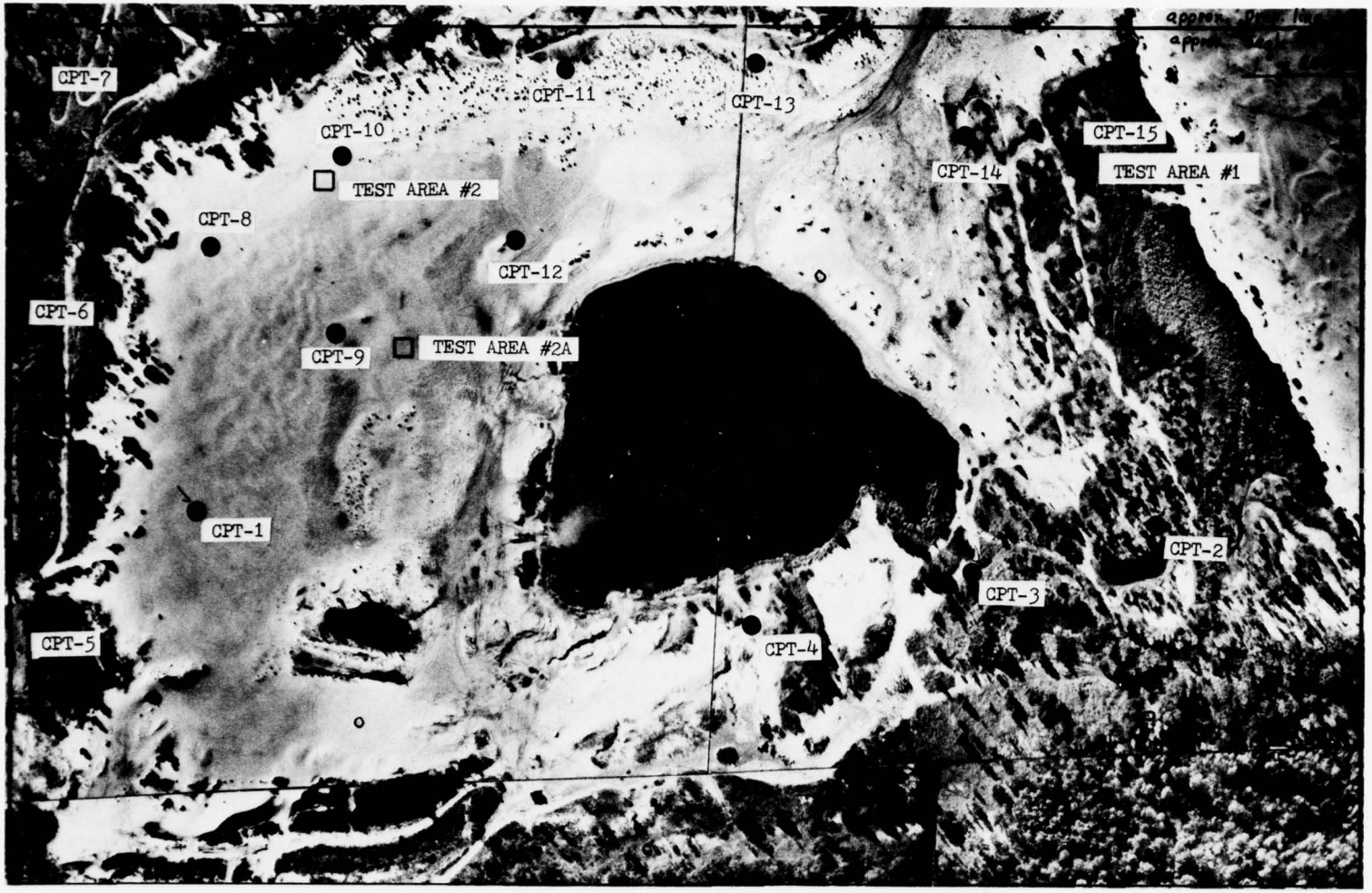

FIGURE 2 - COMPOSITE PHOTO OF AREA PROPOSED FOR HIDDEN LAKES DEVELOPMENT, SHOWING INITIAL SURVEY CONE PENETRATION TEST LOCATIONS AND THE SELECTED TEST AREAS

looking SW W NNW

(a) View of Hidden Lakes tailings area showing vehicles working in Test Area #2A

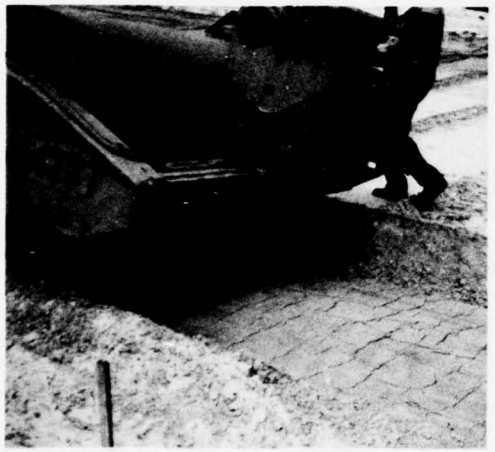

(b) Example of large settlement induced by rolling with BROS VP-20D, 1st pass (31 Aug 76)

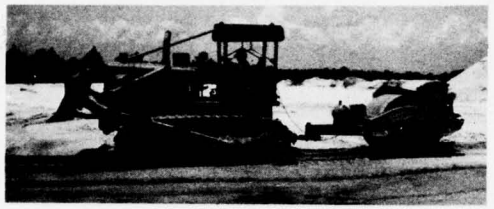

c) Dozer pulling BROS VP-20D, 2nd pass

(d) Tape-to-ground indicates settlement across center section of Test Area #2A after about 6 roller passes

FIGURE - 3

VIBRATORY ROLLER COMPACTION AND RESULTING SETTLEMENT IN TEST AREA #2A

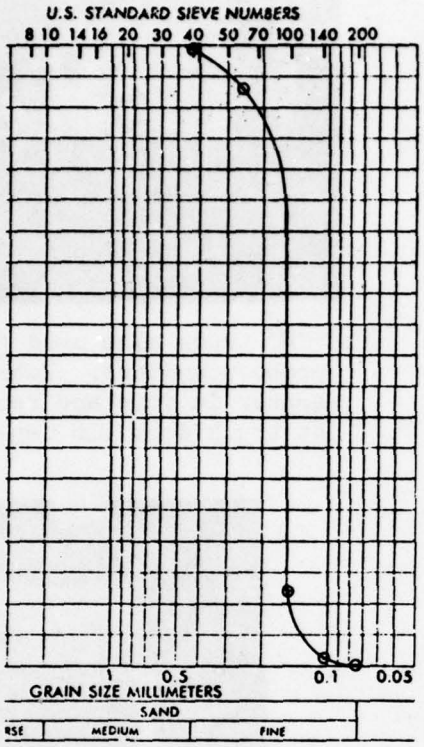

TABLE 1 - RELATIVE DENSITY RESULTS
FROM AREA #2 TEST PIT TESTS

Date	Test No.	Depth (ft)	Dry densities (pcf) in-place	lab max	lab min	D_r	q_c (tsf) range**
24 Aug	1	0.2	101.5	(102.8)*	(87.7)	93%	no data
pit a	2	0.7	101.8	102.8	87.7	95%	11-13
	3	1.2	100.2	(102.7)	(87.6)	86%	14-16
	4	2.0	100.2	"	"	86%	14-22
	5	3.0	96.1	"	"	60%	16-22
	6	3.8	(too wet)	102.5	87.5	--	--
26 Aug	7	0.8	99.9	(102.7)	(87.6)	84%	12-14
pit b	8	1.3	95.7	"	"	58%	14-18
	9	2.1	99.4	"	"	81%	14-22
	10	3.2	95.9	"	"	59%	16-27
	11	4.2	97.3	"	"	68%	16-22
	12	5.2	97.6	104.9	89.2	57%	12-20
	13	6.2	101.5	(")	(")	81%	10-20
	14	7.2	95.6	"	"	45%	6-14

**From 4 CPTs at corners of test area

*Max and min values in ( ) assumed on basis of 3 tests made

FIGURE 4 - AVERAGE SIEVE ANALYSIS GRAIN SIZE DISTRIBUTION OF THE TAILINGS SAND

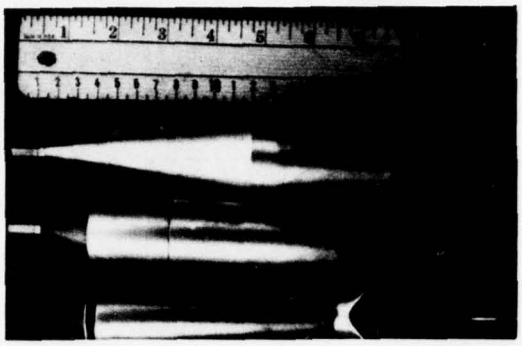

(a) Top to bottom: Wissa and UF pore pressure sounding probes, Dutch mantle CPT cone tip -- all used in this investigation

(b) CPT truck also used for pp probe soundings. Note generator in fore and recorder at truck door (16 Sep 76)

(d) Dozer easily worked itself into sinking 2 ft (operator holding 4 ft rule) in Test Area #1. Sand partly liquefied into "rolling" for c. 15 ft radius around moving dozer. (16 Sep)

(c) Saturated pp probe covered with taped, plastic water bag and then lowered into hole dug to GWL before beginning sounding (16 Sep)

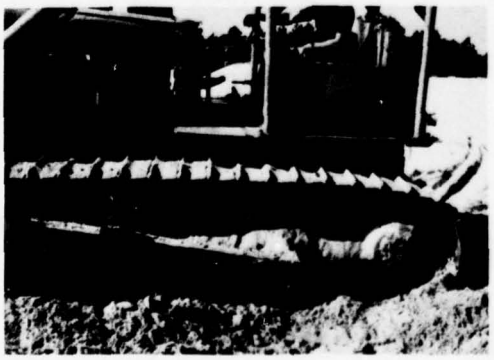

(e) Working, twisting dozer could not produce evidence of ground instability in Test Area #2A, after vibratory roller compaction. (17 Sep 76)

FIGURE - 5

ILLUSTRATIONS OF THE USE OF THE PORE PRESSURE PROBES AND THE CONDITION OF THE TEST AREAS WHERE USED

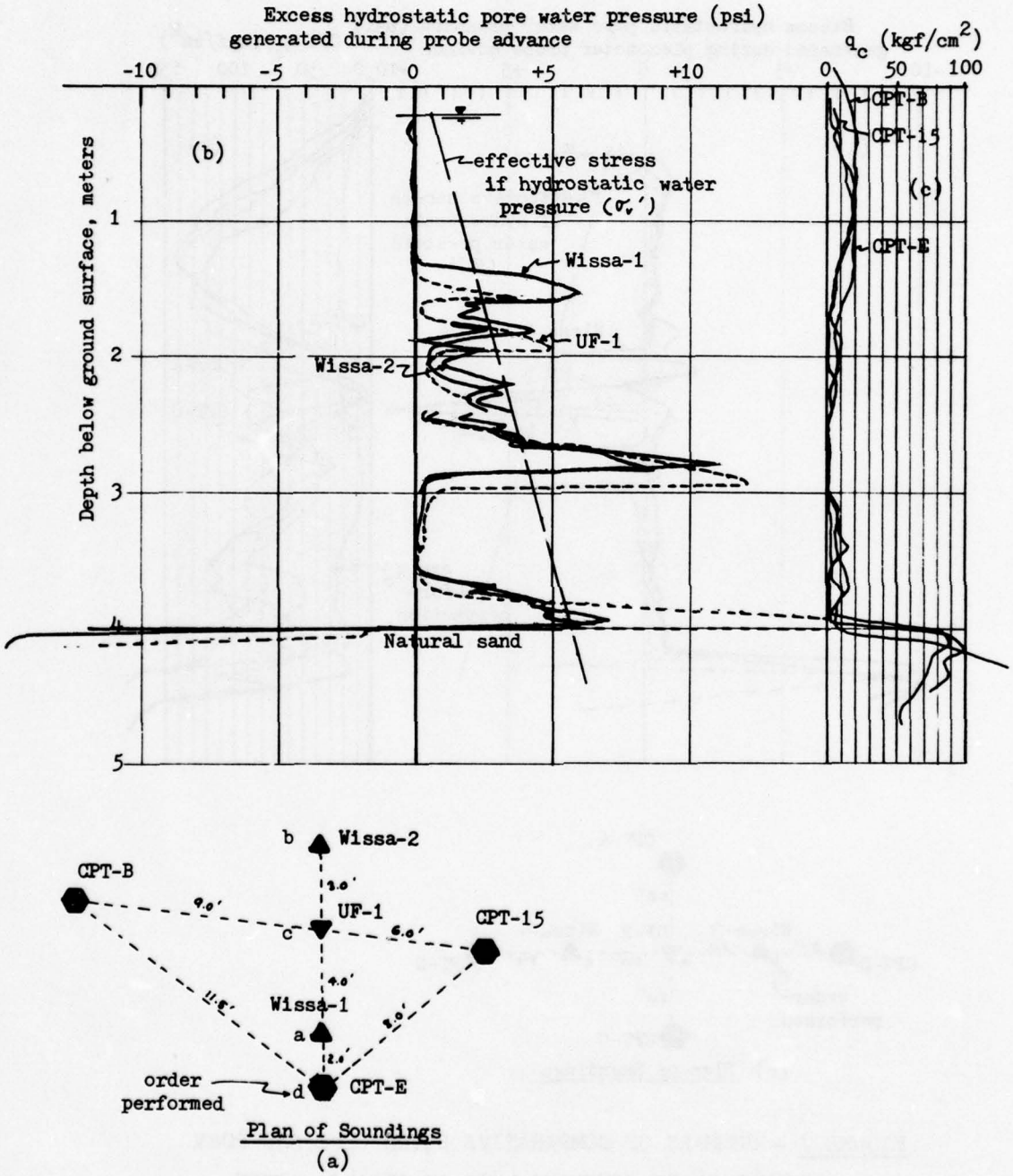

FIGURE 6 - SUMMARY OF COMPARATIVE DUTCH CONE AND PORE PRESSURE PROBE SOUNDING DATA IN AREA #1 WITH UNSTABLE TAILINGS SAND

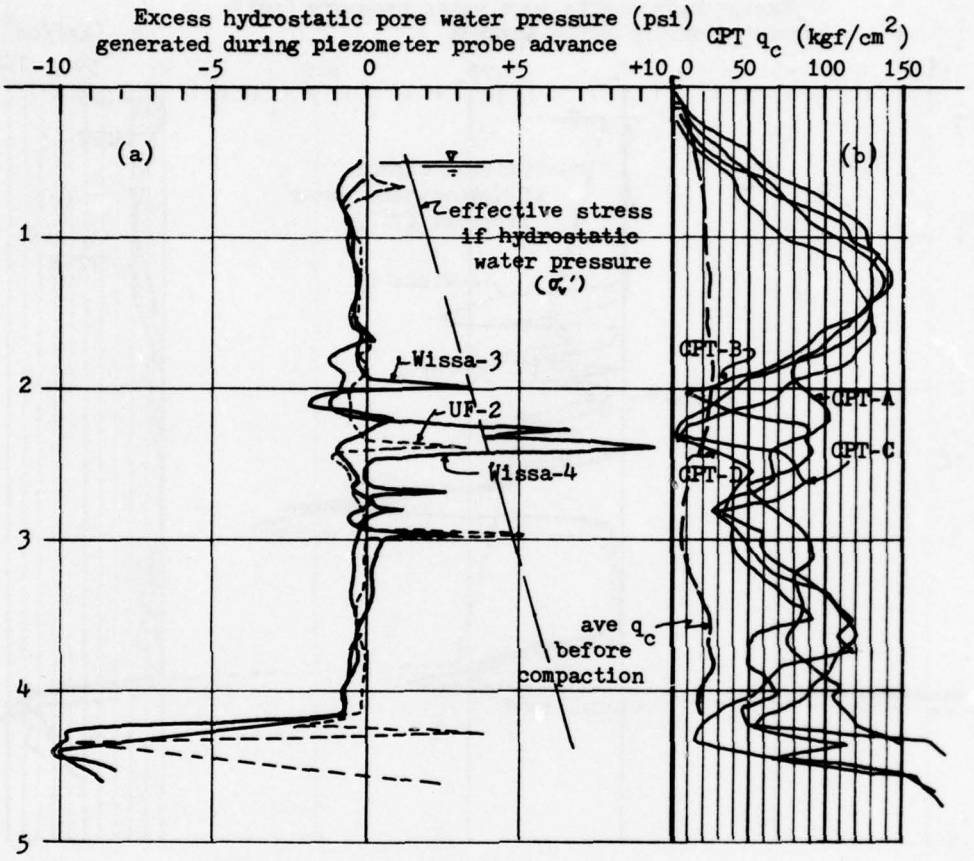

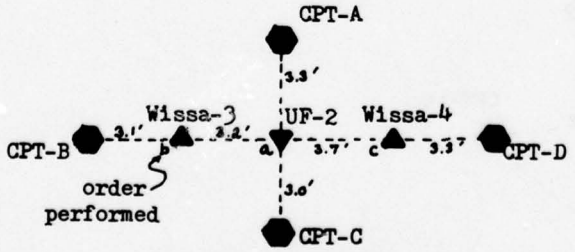

(c) Plan of Soundings

FIGURE 7 - SUMMARY OF COMPARATIVE DUTCH CONE AND PORE PRESSURE PROBE SOUNDING DATA IN AREA 2A AFTER VIBRATORY ROLLER COMPACTION OF TAILINGS SAND

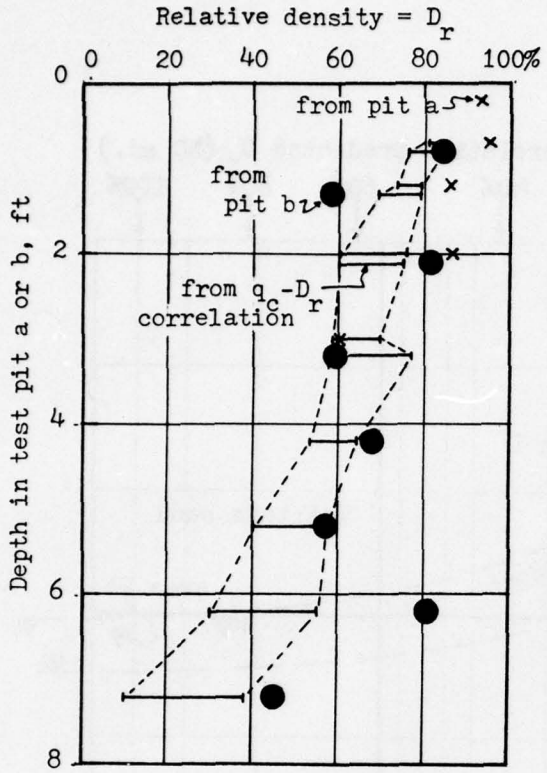

FIGURE 8

COMPARISONS BETWEEN CORRELATION-PREDICTED AND MEASURED RELATIVE DENSITIES AS FOUND IN TEST AREA 2

TABLE 2 - AVERAGE# DATA FROM SELECTED POINTS IN FIGURES 6 AND 7

Test area	Depth (m)	σ_v' (psi)	q_c (psi)	Δu (psi)	$\Delta u/\sigma_v'$	q_c/σ_v'	Notes
1	0.7	1.2	256	-0.1	-0.08	213	
	1.55	2.4	80*	4.9	2.04	33	*No CPT-E
	1.8	2.7	71	3.2	1.19	26	
	2.3	3.4	56	2.2	0.65	16½	
	2.8	4.05	25	9.0	2.22	6.2	
	3.2	4.55	100	0.3	0.07	22	
	3.9	5.6	46	6.5	1.16	8.2	Wissa
	"	"	25	15.0	2.68	4.5	UF
	4.1	5.8	1280	-15.0	-2.59	221	Nat. sd.
2A	0.8	1.7	1066	-0.7	-0.41	627	
	1.3	2.45	1780	-0.3	-0.12	726	
	1.8	3.1	1350	-0.5	-0.16	435	
	2.3	3.8	42	7	1.84	11	
	2.6	4.2	995	-0.3	-0.07	237	
	3.3	5.2	1138	-0.2	-0.06	219	
	3.6	5.65	1350	-0.3	-0.05	239	
	4.3	6.6	1500	-10	-1.52	227	Nat. sd.

#of both probes, could not distinguish between probes from the available data

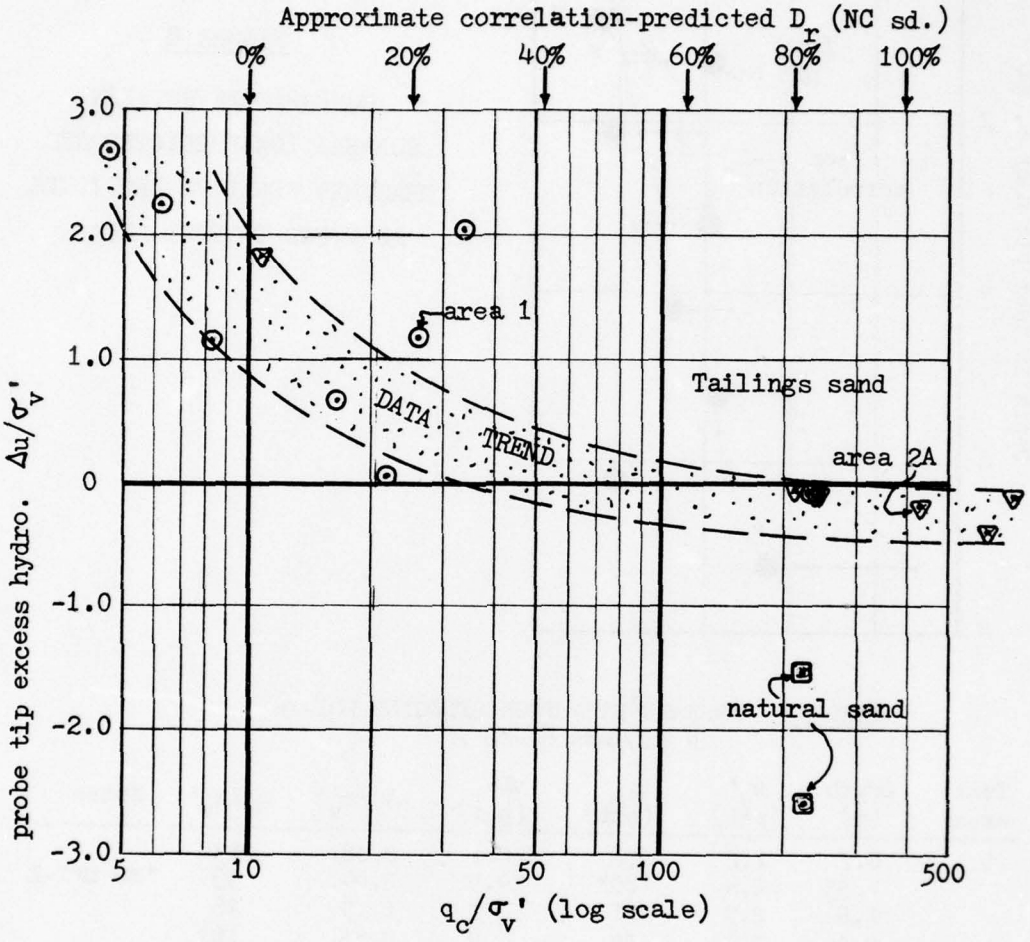

FIGURE 9 - AVERAGED TEST AREA 1 AND 2A DATA SHOWING TREND OF PORE PRESSURES GENERATED AT PROBE TIP VS. STATIC CONE BEARING CAPACITY AND RELATIVE DENSITY (see Table 2)

APPENDIX I

DETAILED LOGS FROM PROBE AND CPT SOUNDINGS

IN TEST AREA 1

Probe: Wissa-1
Wissa-2
UF-1

CPT: -15
-B
-E

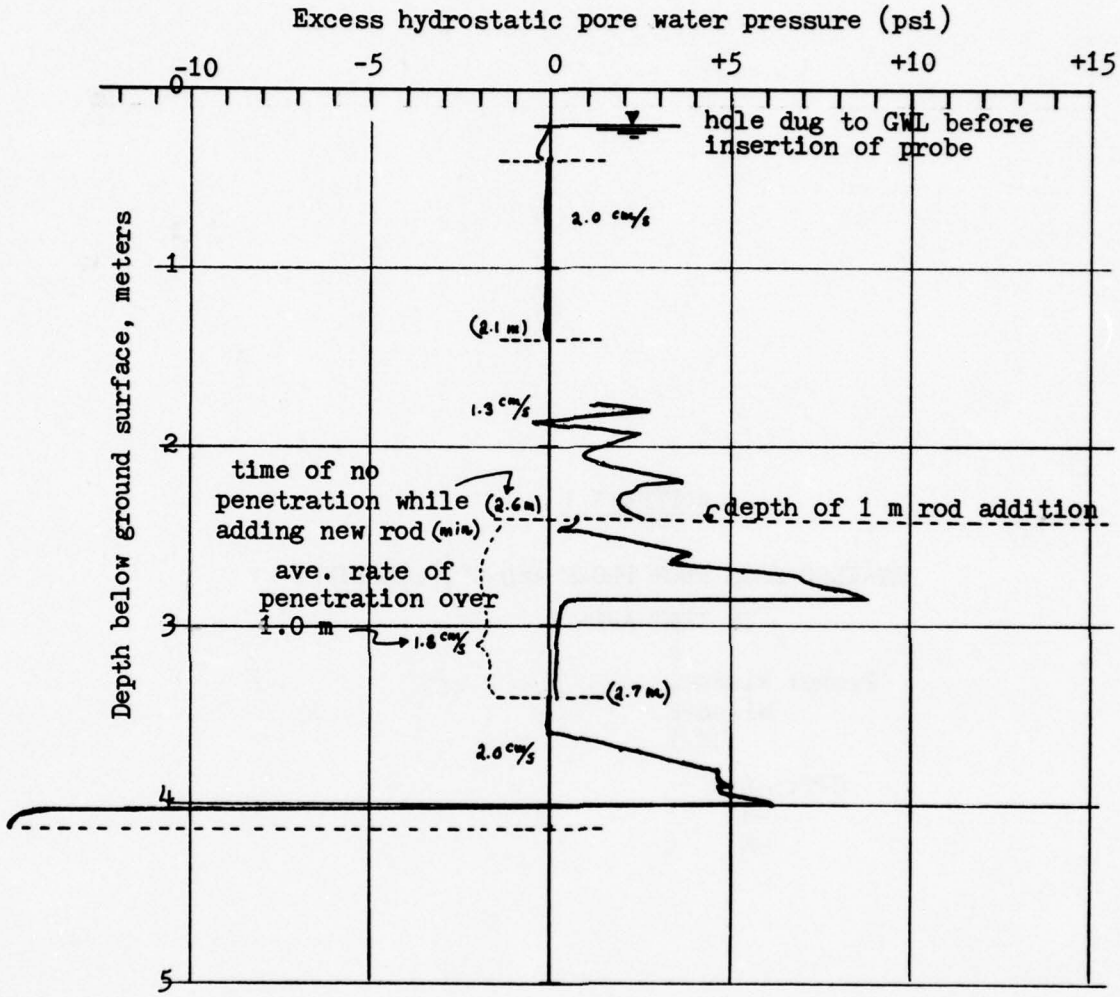

Area 1 -- Wissa-1 sounding

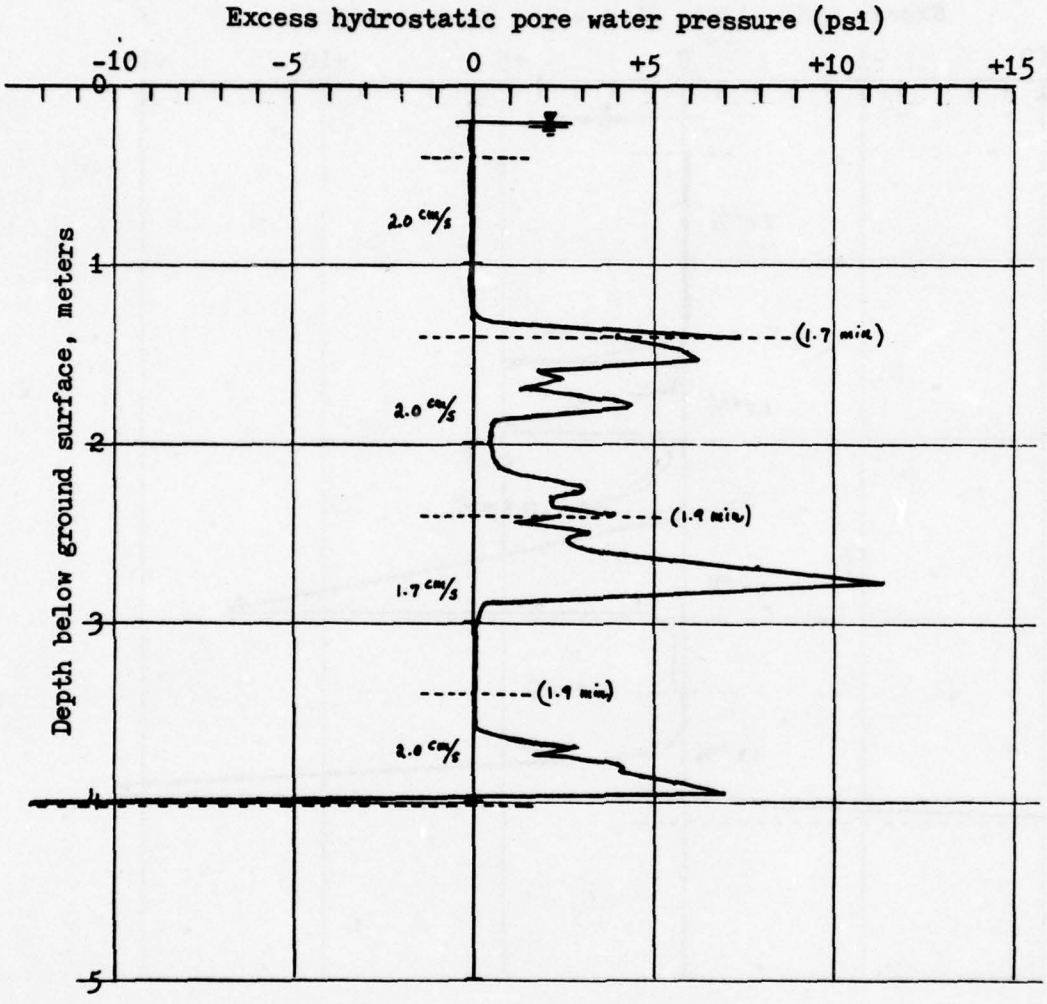

Area 1 -- Wissa-2 sounding

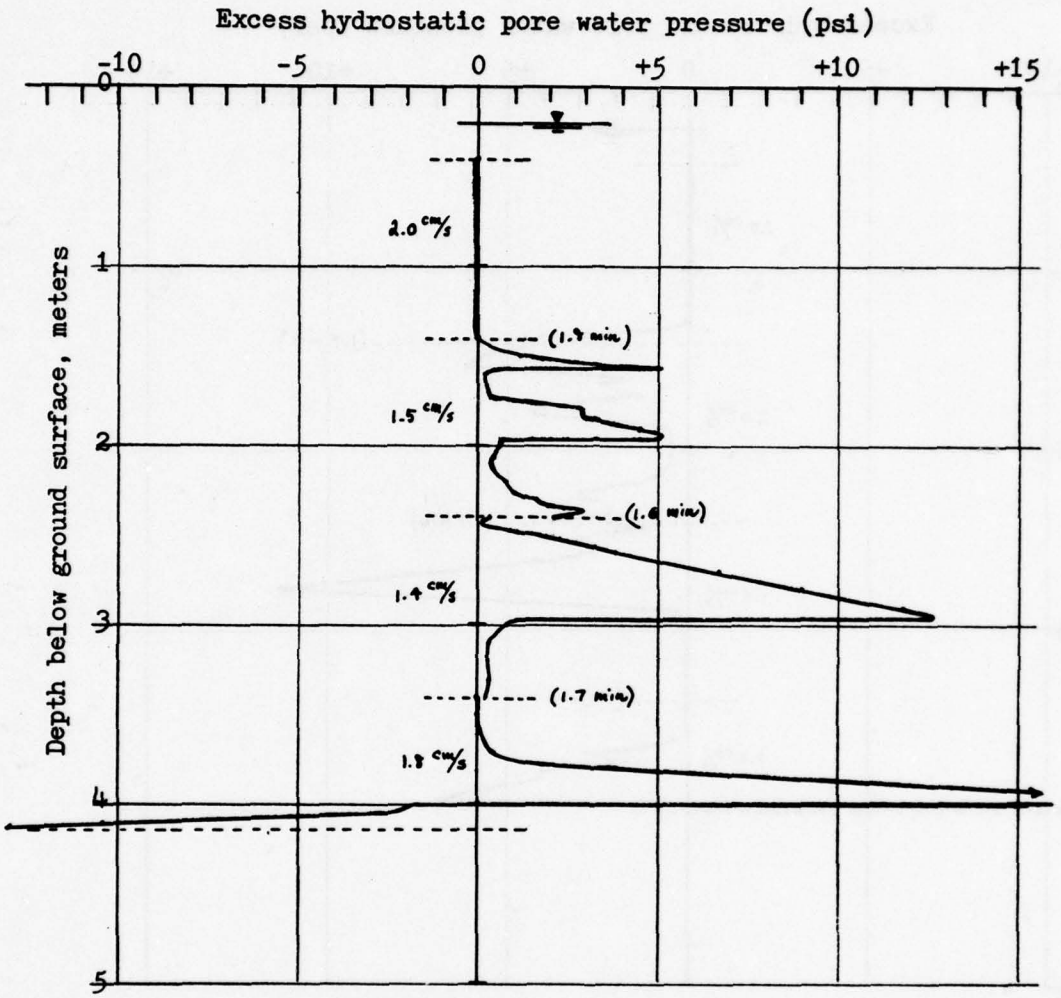

Area 1 -- UF-1 sounding

UNIVERSITY OF FLORIDA
SOIL MECHANICS LABORATORY - FIELD UNIT

LOG OF DUTCH FRICTION-CONE SOUNDING
(10 cm^2, 60°, steel point adv. 2 cm/sec)

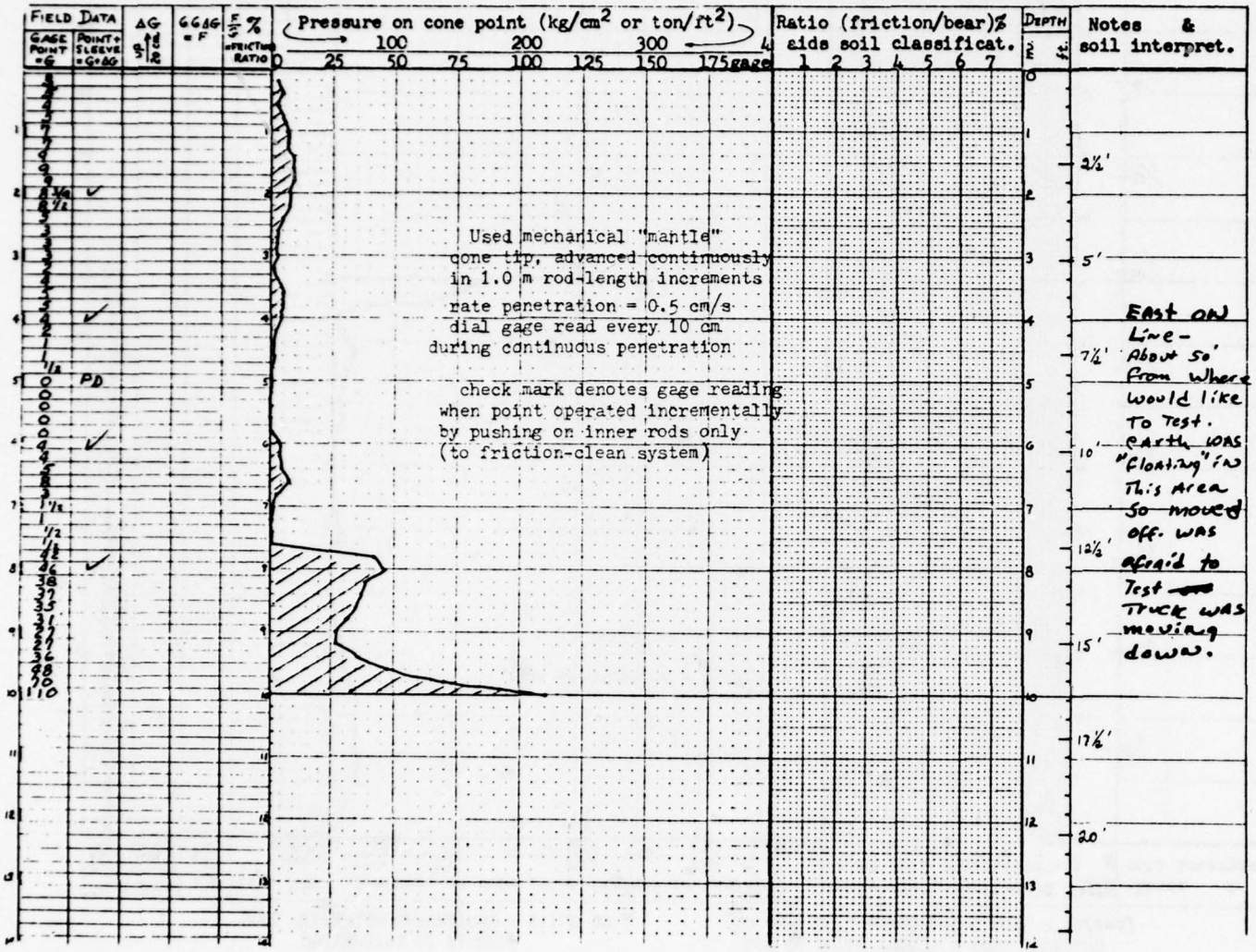

Project #164 Cone No. 15 Location JAX. By: WJW-JWA Date 8-6-76 Pi of

UNIVERSITY OF FLORIDA
SOIL MECHANICS LABORATORY - FIELD UNIT

LOG OF DUTCH FRICTION-CONE SOUNDING
(10 cm^2, 60°, steel point adv. 2 cm/sec)

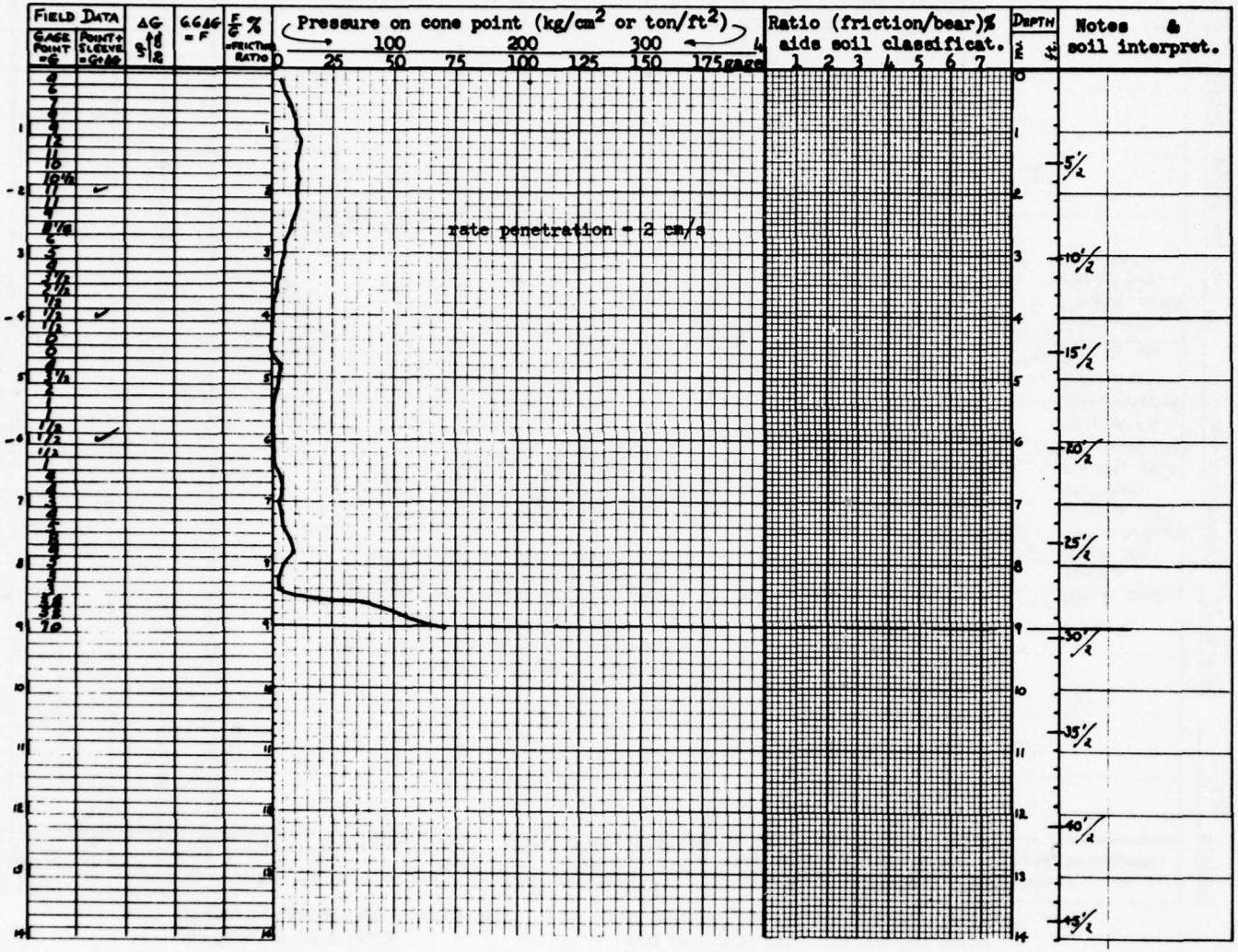

Project #164 Cone No. B Location TEST SITE 1 By: WJW. JUPA Date 8-10-76 Pg. of

UNIVERSITY OF FLORIDA
SOIL MECHANICS LABORATORY - FIELD UNIT

LOG OF DUTCH FRICTION-CONE SOUNDING
(10 cm^2, 60°, steel point adv. 2 cm/sec)

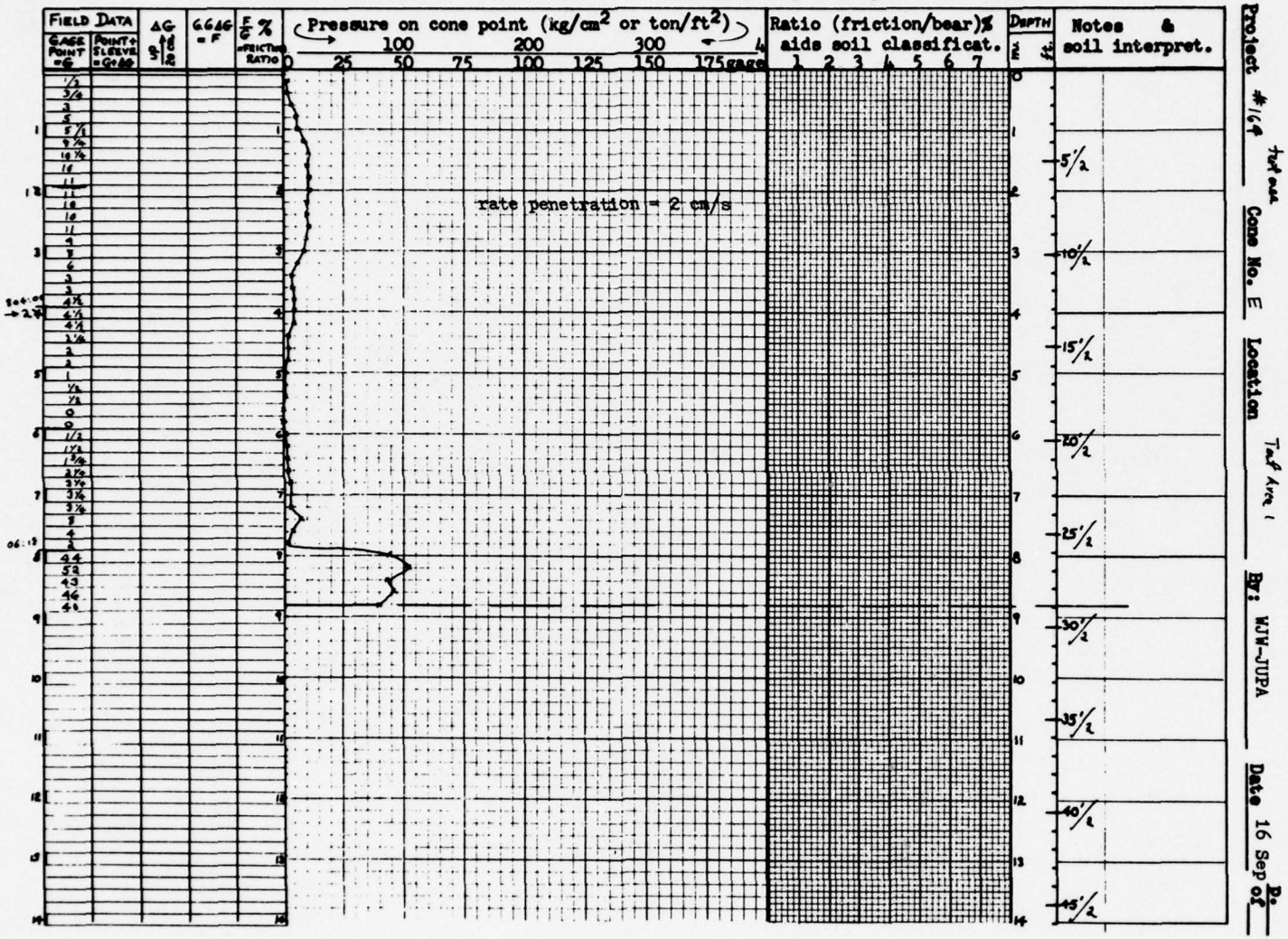

Project #164 Turf exp. Cone No. E Location Turf Area 1 By: WJW-JUPA Date 16 Sep Pg of

APPENDIX II

DETAILED LOGS FROM PROBE AND CPT SOUNDINGS IN TEST AREA 2A

Probes: UF-2
Wissa-3
Wissa-4

CPTs: -A
-B
-C
-D

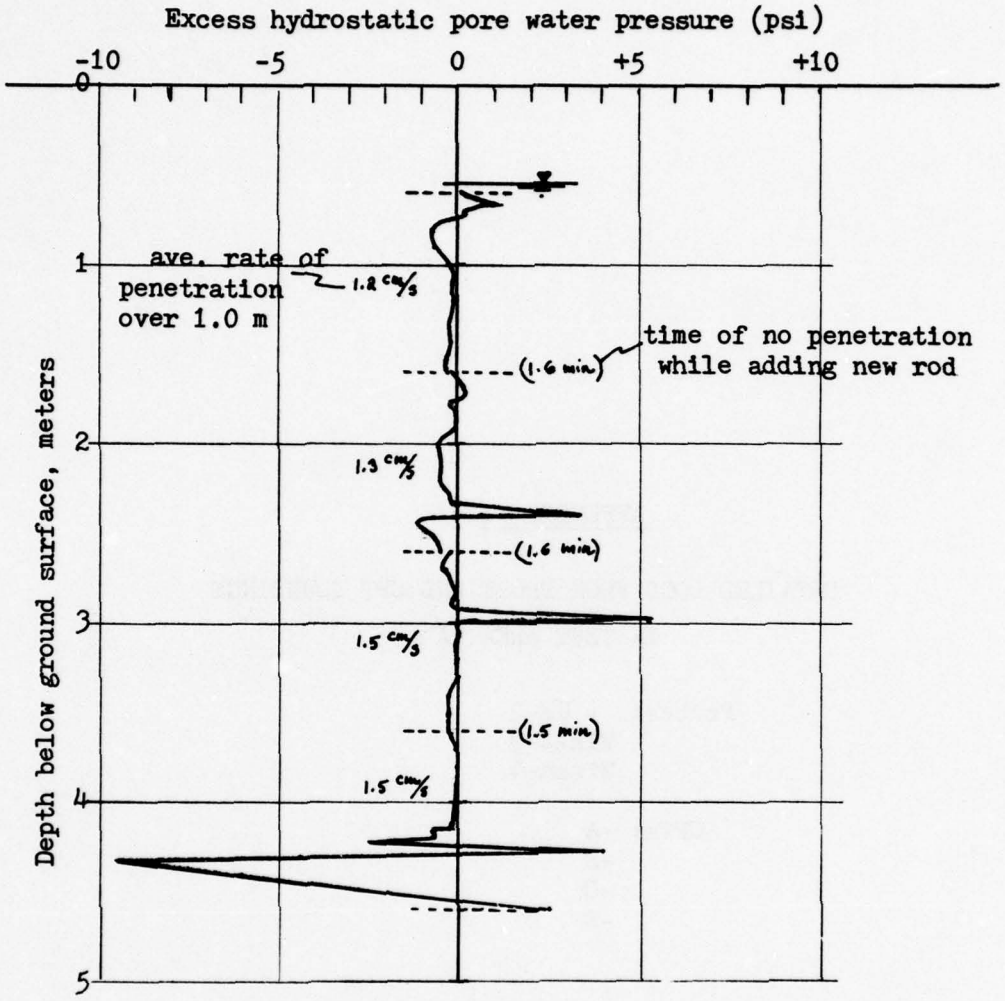

Test Area 2A -- UF-2 sounding

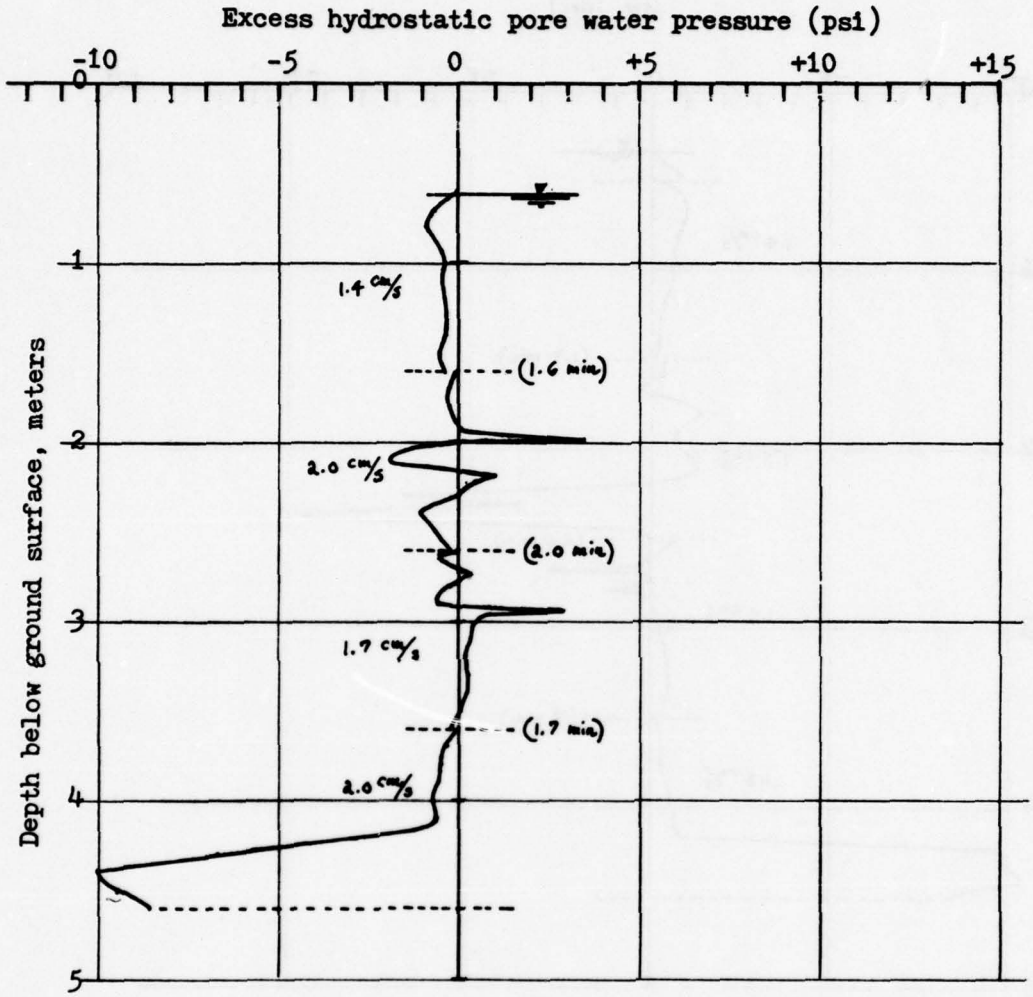

Test area 2A -- Wissa-3 sounding

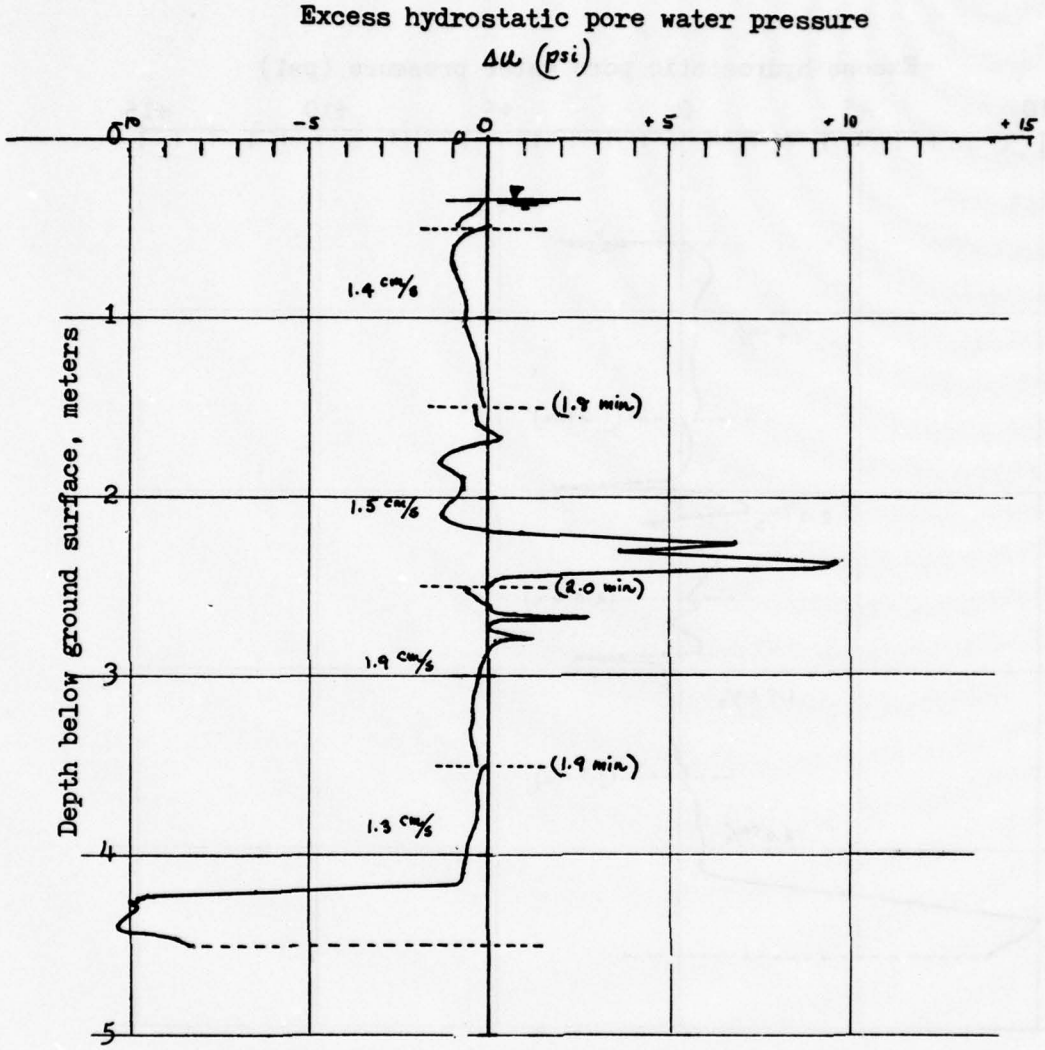

Test area 2A -- Wissa-4 sounding

UNIVERSITY OF FLORIDA
SOIL MECHANICS LABORATORY - FIELD UNIT

LOG OF DUTCH FRICTION-CONE SOUNDING
(10 cm^2, 60°, steel point adv. 2 cm/sec)

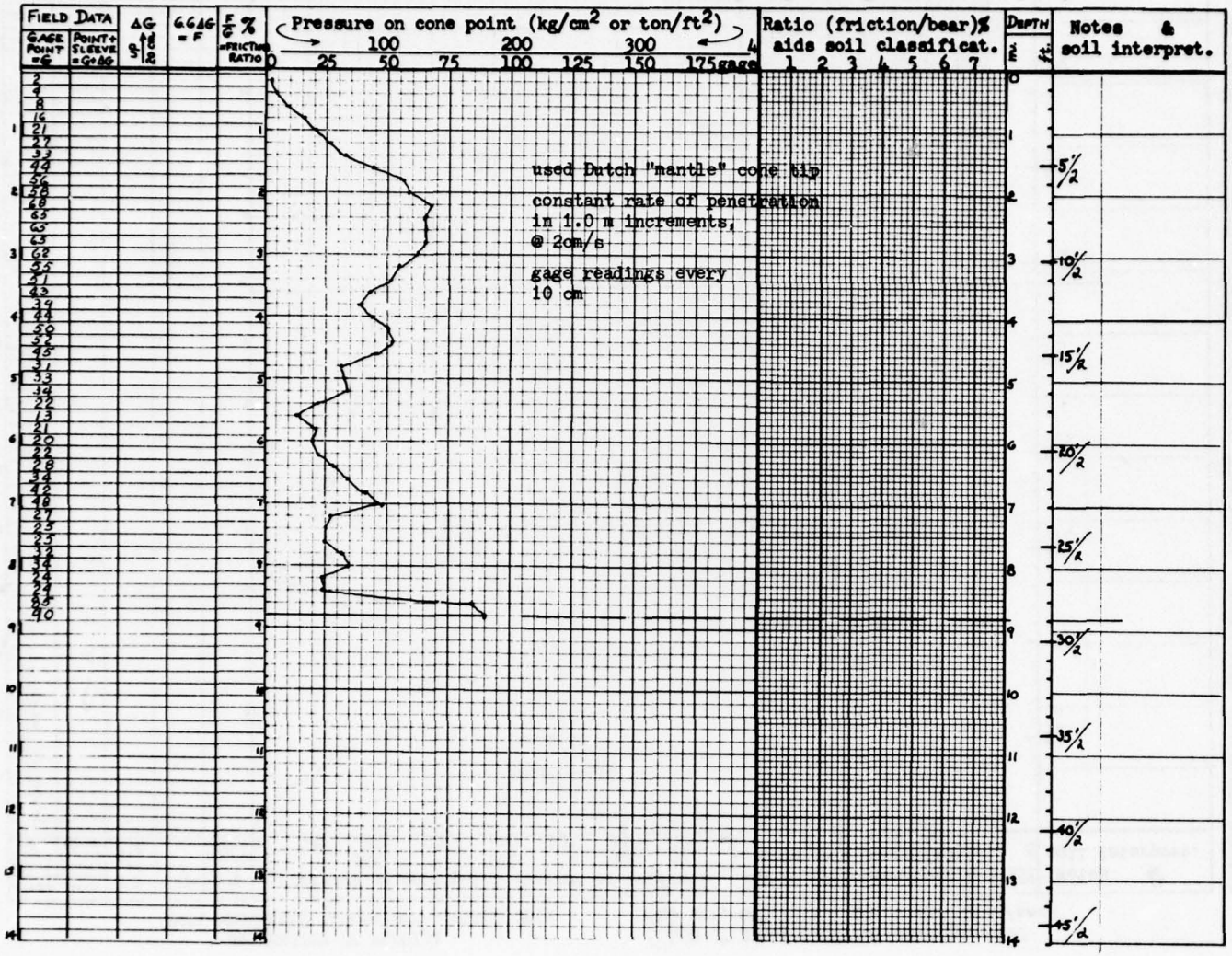

Project # 164 Cone No. A Location Test site 2-A By: WJW-JP Date 9-12-74 Pg. of

UNIVERSITY OF FLORIDA
SOIL MECHANICS LABORATORY - FIELD UNIT

LOG OF DUTCH FRICTION-CONE SOUNDING
(10 cm^2, 60°, steel point adv. 2 cm/sec)

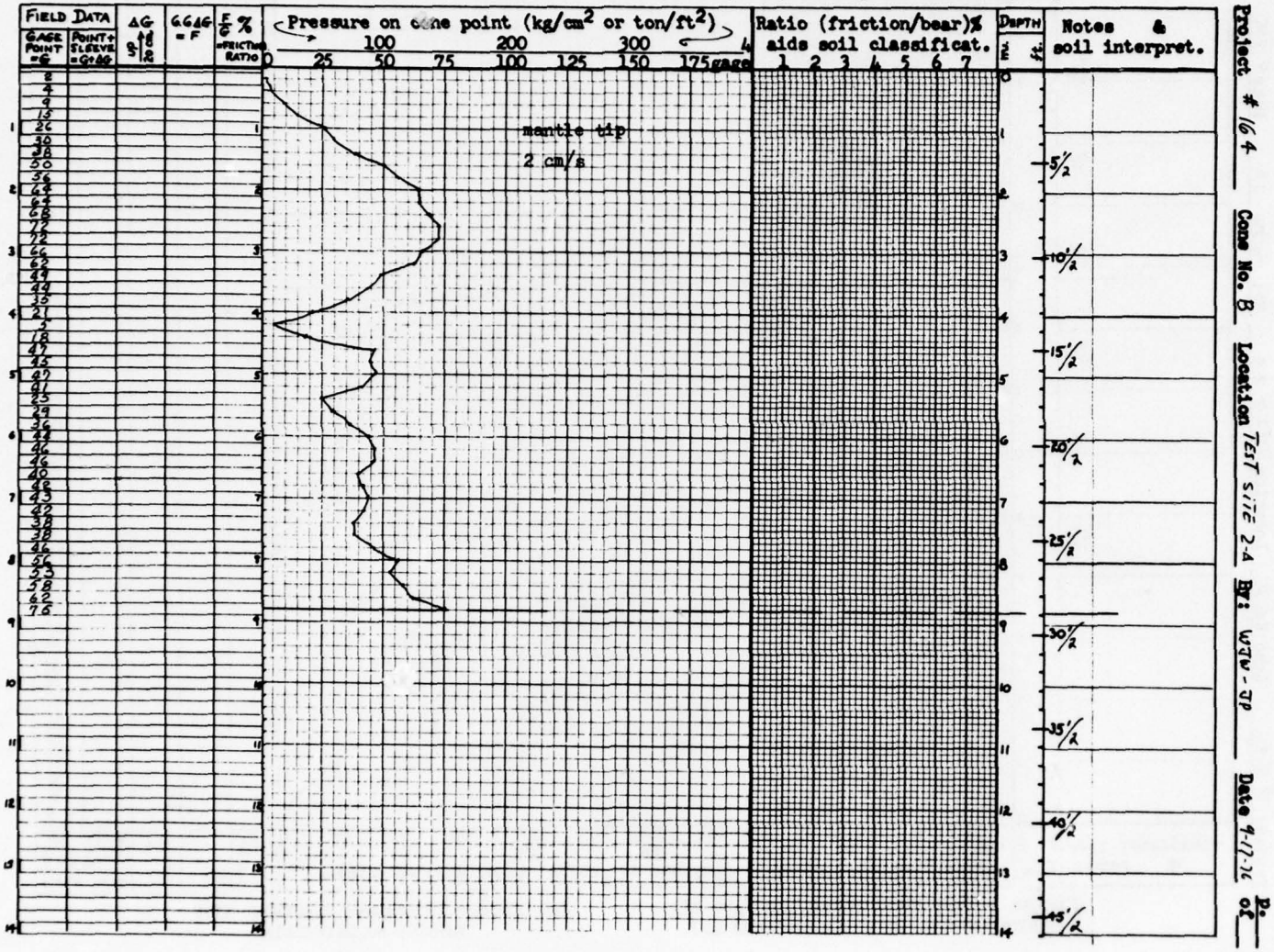

Project # 164 Cone No. B Location TEST SITE 2-4 By: WJW - JP Date 4-17-74 P. of

UNIVERSITY OF FLORIDA
SOIL MECHANICS LABORATORY - FIELD UNIT

LOG OF DUTCH FRICTION-CONE SOUNDING
(10 cm^2, 60°, steel point adv. 2 cm/sec)

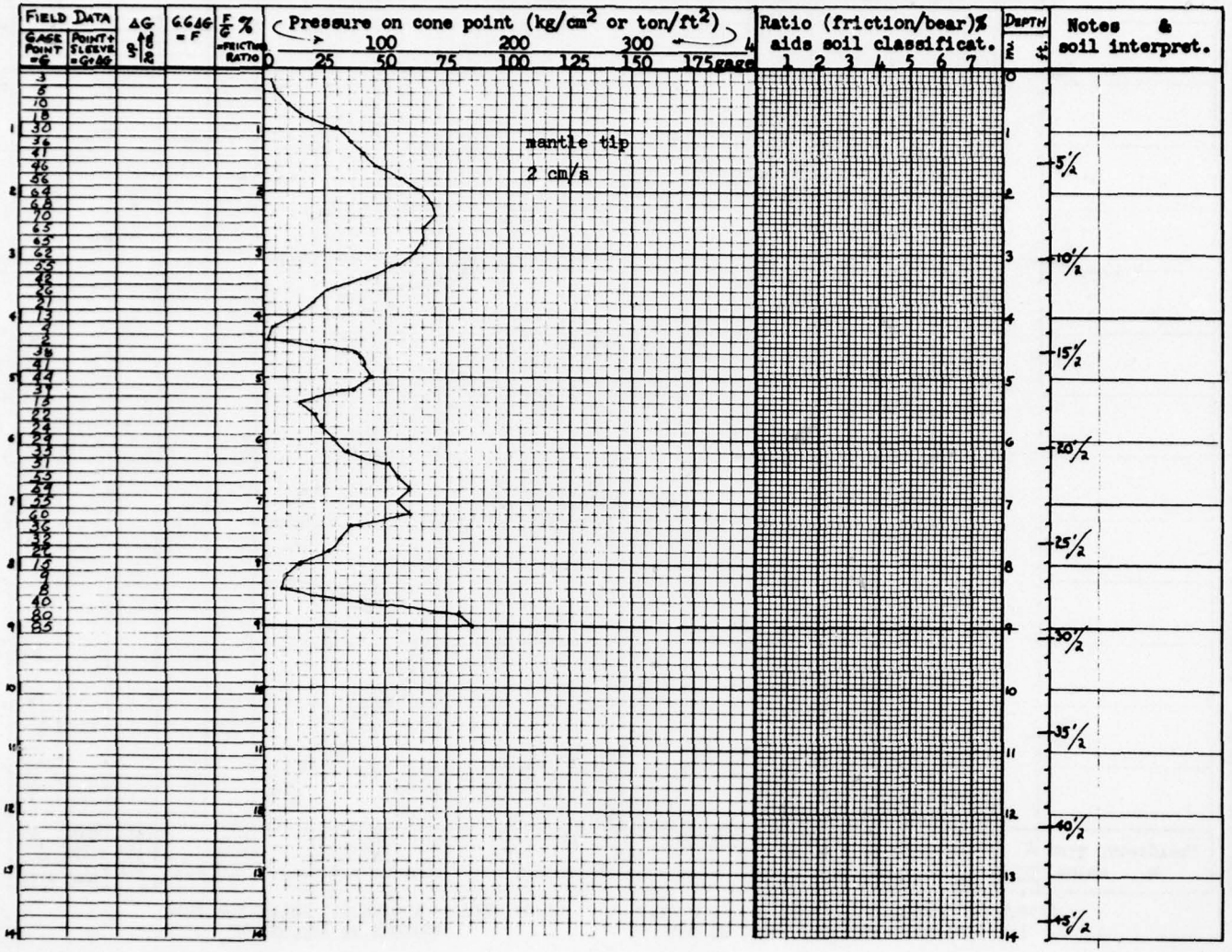

Project #164 Cone No. C Location TEST SITE 2-A By: WJW-JP Date 9-12-74 Pg. 1 of 1

UNIVERSITY OF FLORIDA
SOIL MECHANICS LABORATORY - FIELD UNIT

LOG OF DUTCH FRICTION-CONE SOUNDING
(10 cm^2, 60°, steel point adv. 2 cm/sec)

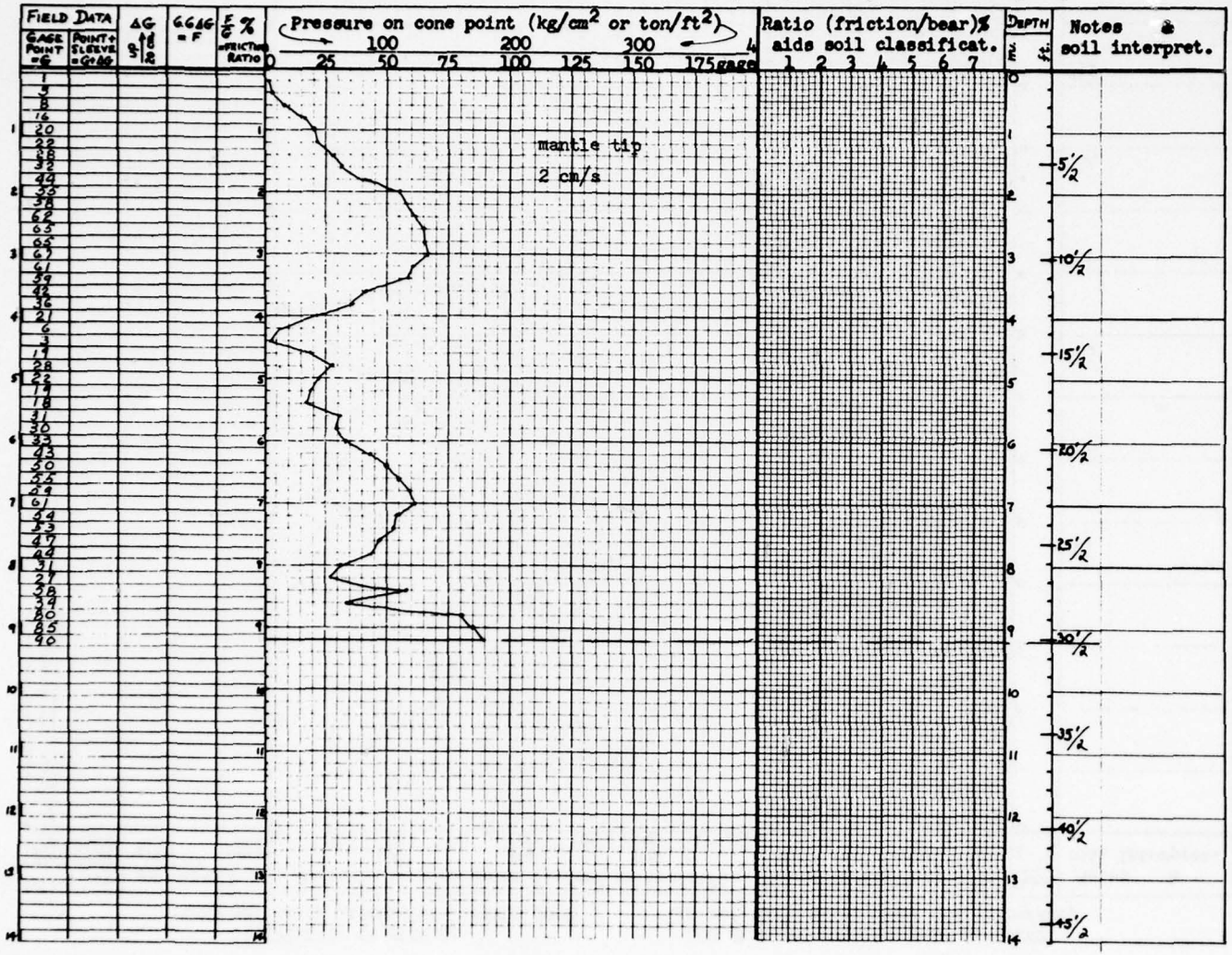

Project #164 Cone No. D Location TEST SITE 2-A By: WJW - JP Date 9-12-74 P. of

APPENDIX III

THE MOST RECENT q_c-D_r CORRELATION AND ITS BASIS

AN UPDATED CORRELATION
BETWEEN RELATIVE DENSITY, D_r, & FUGRO-TYPE ELECTRIC CONE BEARING, q_c

1. NEW CORRELATION

Figure 1 herein presents the updated correlation in the form of curves of q_c vs. vertical effective stress, σ_v', both in kgf/cm^2, at six levels of D_r. Knowing q_c from static sounding (ASTM D-3441-75T) data, and estimating σ_v' from depth and water table information, permits the user to enter Fig. 1 and obtain an estimate of D_r.

The correlation applies to normally consolidated (NC), uncemented, primarily quartz, geologically recent, saturated, fine SP sands insitu, when using the Fugro-type, 10 cm^2, 60°, cylindrical tip, advanced continuously at 2 cm/s.

The following equations (1) or (2) express the Fig. 1 correlation:

$$q_c = C_o \sigma_v'^{C_1} \exp (C_2 D_r\%/100) \quad \ldots\ldots\ldots (1)$$

$$D_r\% = \frac{1}{C_2} \ln (q_c/C_o \sigma_v'^{C_1}) 100\% \quad \ldots\ldots\ldots (2)$$

with: $C_o = 12.31$
$C_1 = 0.71$
$C_2 = 2.91$

They result from a statistical analysis of the special sets of new experiments that form the basis of the correlation, as discussed in 2. below.

Figure 1 also shows, by means of light dashed lines, the previous correlation prepared in 1971 for private distribution and later published as Figure 10 in Schmertmann (1975). We found that a correlation in the form of the above eqns. (1) and (2) also fit well the data base for this previous correlation, but with different C values. Note the considerable adjustment of the curves at the high D_r region of the curves. A given q_c in these regions now predicts a lower insitu D_r, which matches better with the general offshore experience since 1971.

2. BASIS OF CORRELATION

2.1 Test Chamber: The new data now available to update the subject

correlation comes from 80 additional U. Fla. calibration chamber tests. This chamber permits the vertical insertion of the cone tip along the axis of a cylindrical "sample" 4.0 ft in diameter and 4.0 ft high. Each test involves a separate sample, rained dry into the chamber to obtain a uniform sand with a structure hopefully approximating that common from natural deposition. The chamber then permits triaxial, K_o consolidation of the sand using separate membrane and water pressure systems for the horizontal end planes and the cylindrical vertical plane. The chamber controls permit the operator to maintain either of two sample boundary conditions during the cone tip insertion -- either constant-stress, separately along the vertical and horizontal boundaries, or overall sample constant-volume. See Veismanis (1974) or Laier et. al. (1975) for further description of the U.F. chamber.

2.2 Scope of Tests: The new correlation results primarily from 57 of the additional 80 tests, these 57 performed on two artificial, relatively uncrushable and easily crushable fine sands, at two levels of vertical effective stress (10 and 40 psi), at four levels of relative density (20-80%), at two chamber boundary conditions (constant-stress and constant-volume), and at two levels of water content (air-dry and near-saturated). All tests employed the Fugro electric tip, advanced continuously. We planned the test series to form various groupings, designed to permit a detailed statistical evaluation of these data. This plan included test replications. See Harman (1976) for more statistical details than covered herein.

These 57 tests differed significantly from those available for the 1971 correlation: fine sands instead of medium; inclusion of a crushable sand; relative densities under the previous low of c. 50%; use of the constant-volume boundary condition as well as the previous constant-stress only; and, possibly for the first time in such chamber testing, the use of near-saturated samples as well as the previous air-dry only. Eighteen of the 57 had near-saturated conditions before cone tip insertion.

The remaining 23 new tests also used fine sands, but two naturally occurring ones. Eleven of these 23 had the near-saturated condition. The following Table I lists the scope of the total of 80 tests and the range of the variables included therein.

TABLE I - SCOPE OF THE ADDITIONAL U.F. CHAMBER TESTS **

Sand	Test conditions		No.	Range of D_r (%)		Range of q_c (kgf/cm^2)	
	Boundary	Water	tests	min	max	min	max
1. Ottawa #90 artificial, quartz, rounded, non-crushable D_{60}=0.24, D_{10}=.13mm $\gamma_d$max = 111.7 pcf $\gamma_d$min = 92.8 0.2% -200 sieve	const-σ'	air-dry	14	16	83	15	303
	const-σ'	near-sat (90-100%)*	12	19	80	14	304
	const-V	air-dry	9	20	81	16	428
2. Hilton mines crushed, fine iron mine tailings, angular, qtz + feldspar + mica D_{60}=.30, D_{10}=.15mm $\gamma_d$max = 116.0 pcf $\gamma_d$min = 91.8 3% -200 sieve	const-σ'	air-dry	8	28	86	22	235
	const-σ'	near-sat (87-94%)*	8		86	18	244
	const-V	air-dry	6 / 57	32	84	16	162
3. Edgar Fla. 70-140 sieved sand residue from kaolinite mine, quartz, D_{60}=.17 mm D_{10}=.10mm, 0.9% -200 $\gamma_d$max = 101.1 pcf $\gamma_d$min = 80.3	const-σ'	air-dry	8	34	75	25	211
		near-sat (94-95%)*	3	33	67	23	195
4. Ried Bedford Dredged from Miss. R., WES std. sand, D_{60}=.30, D_{10}=.15mm $\gamma_d$max = 107.1 pcf $\gamma_d$min = 88.7, 1.2% -200	const-σ'	air-dry	4	25	81	16	243
		near-sat (97-98%)*	8 / 23	27	81	20	255

*This range the ave. % saturation for entire sample, using estimated dry weight of sand in chamber. Sat. believed higher along axis of cone penetration.

**Two levels of σ_v', 0.5 and 2.8 kgf/cm, for all groups

2.3 Relative densities: The accuracy of any D_r correlation depends in part on the method(s) used to determine the maximum and minimum and test dry unit weights.

We determined the max and min values using two methods: the ASTM D-2049-69 method, dry, using an electrostatic vibrating table, and the Burmister (1948) method using a 200ml plastic mold and a Burgess "Vibrotool" and layer compaction. We made at least two determinations with each method and the values reported in Table I represent the extremes we found reproducible. In the case of the Ried Bedford sand we used the values for max and min supplied by the Waterways Experiment Station, from where we obtained this sand. Professor Ken Lee of UCLA also tested these sands for extreme unit weights using his own methods, both wet and dry. All of his extreme values differ from those in Table I by an ave. of 0.6 pcf, with a max of 1.2 pcf, without pattern.

For each chamber test in which we tested with dry sand we weighed all the sand on its removal after the test and divided by the total volume of the sample (about 50 ft^3) at the time of cone tip insertion (after consolidation). We used this average sample dry unit weight in the calculation for D_r. For the near-saturated tests we assumed the dry weight of the sand as the average of the many previous tests wherein we had actually weighed the sand.

Prior to all these 80 tests we made an extensive study of the uniformity with which we cast a sample using our raining method from a fixed-elev. hopper. Caillemer (1975) demonstrated a std. deviation in dry unit weight of about 1.0 pcf in both the radial and vertical directions within the sample. This probably exceeds the uniformity of any equal volume of sand in a natural deposit, and matches our ability to determine any insitu density.

3. OTHER RESULTS FROM STATISTICAL STUDIES

3.1 The Important Variables: Analyses of variance performed by Dr. Mehmet Tumay for different grids of data, including some from previous chamber testing, showed the following Table II descending order of importance for the independent variables studied, when determining q_c:

TABLE II - RELATIVE IMPORTANCE OF TEST VARIABLES DETERMINING q_c

A. By far most important:

1. Vertical effective stress

   For the NC tests the vertical eff. stress proved of slightly greater significance than either the horiz. or octahedral effective stresses. Of course, we can also more easily estimate the vertical.

2. Relative density (of almost equal importance)

B. Considerably less important than A.

3. Interaction between 1. and 2.

4. State of overconsolidation, the OCR

C. The rest of much less importance, with descending order less well defined.

5. Type of sand

6. Interaction between 2. and 5., which likely represents a measure of particle packing, or structure.

7. Boundary condition

8. Degree of saturation (dry or near-sat)

9. Type of cone tip

10. Replication of tests

The above findings have practical implications. The relatively minor importance of sand type suggests that any correlation should provide about equal accuracy in a broad band of soils. The similar finding for boundary condition indicates that the 4 ft chamber samples probably provide an adequate model of insitu conditions. The similar finding for saturation indicates we can use the results from air-dry test samples (much easier to prepare and test) to estimate the results for the saturated state. The minor importance of the cone tip type, electrical or mechanical, means the correlation may prove adequate also for data from mechanical tips. The least importance of replication means the subject series of chamber tests had more than adequate reproducability.

However, we cannot ignore the state of overconsolidation (OCR), or in effect the horizontal effective stress condition if other than NC.

3.2 Effect of Sand Crushability (compressibility): Figure 2 presents the results of regression analyses from the two fine sands, dry, with crushability extremes -- Ottawa and Hilton. Both sets have high correlation coefficients, which also applies to the sets discussed later. The more crushable, but also more angular, Hilton has higher q_c for a given D_r until $\sigma_v' = 1.0$ kgf/cm^2. It probably has a higher ϕ' at low stress. At higher stress levels its crushability allows the cone to enter more easily, thus producing a lower q_c at any given D_r. Figure 2 describes the constant-stress boundary test results only.

Figure 3 presents the comparative regression results from the same two sands, this time tested with a constant-volume boundary. When the boundary cannot change volume the lack of crushability causes q_c in the Ottawa sand to increase greatly.

3.3 Effect of Boundary Condition: Insitu we probably have a boundary condition around the perimeter of any imagined 4' diameter and 4' high cylindrical specimen, subjected to the volume displacement of the penetrating cone and overhead rods, that lies somewhere between constant-stress and constant-volume. We therefore used both boundary conditions and attempted an interpolation.

3.3.1 Non-crushable (Ottawa) sand: Figure 4 compares the regression results on this sand using both boundary conditions. The effect of the constant-V confinement has significance at all $D_r \succ 20\%$, becoming very pronounced at high D_r. The combination of high density particle packing and incompressibility forces very high q_c before the grains will crush to make room for the cone and rods.

3.3.2 Crushable (Hilton) sand: Figure 5 compares the regression results for this sand using both boundary conditions. Note the relatively minor importance of boundary condition. At constant-V the crushable (compressible) nature of the sand even cause a reduction in q_c compared to the constant-stress condition. Only at high stress and D_r does q_c require an increase to force the volume displacement of the cone and rods.

3.4 Effect of Saturation: The penetration of the cone and rods can produce a complicated, moving, pore pressure field around the advancing tip,

generally involving both + and - pore water pressures (Schmertmann, 1974). Effective stresses during penetration probably change as a result of this pore pressure field. Figure 6 shows the effects of near-saturation on the regression analysis results from air-dry and near-saturated Ottawa sand. For this relatively uncrushable sand, saturation had only a minor effect on q_c.

Although not sufficient in scope for a similar comparative regression analysis, the near-saturated tests on Hilton sand showed an average q_c reduction of about 30% at $\sigma_v' = 0.5$ kgf/cm^2 and at all D_r, compared to matching air-dry tests. It appears that increasing sand compressibility causes significant reduction in q_c when changing from the air-dry to the near-saturated condition.

3.5 The final, combined correlation curves: As presented by Fig. 1 and equations (1) and (2), the final regression analysis included all the 57 tests on NC Ottawa and Hilton sands. We used all the available near-saturated and air-dry test comparisons to form a basis for correcting the more numerous dry tests to the desired saturated state expected insitu. Also, after some study of alternatives, we chose the boundary condition point 1/3 between constant-stress and constant-volume, nearer constant-stress, as our best estimate of the average insitu condition.

4. D_r PREDICTION ACCURACY

4.1 Ottawa & Hilton sands: Analysis of all the absolute differences $|D_r$ (predicted from Fig. 1) - D_r (actual in test)$|$ produces a standard error of about 5% for both sands, at both boundary and saturation conditions. This represents the best possible prediction accuracy.

4.2 Edgar & Bedford sands: The chamber test results from these sands did not figure in the regression analyses that produced the Fig. 1 correlation. Instead, we used them as a further check on the D_r prediction accuracy. Figure 7 presents a histogram of the error ratio, in %, including both near saturated (range of 95-98% for entire sample) and air-dry, from both sands. Both sands produced data similar enough for inclusion in a single histogram. These data suggest an approximate normal distribution of error, with a std. deviation in $(D_{r,pred.} - D_{r,\ meas})/D_{r,meas}$ of about 10%.

4.3 Field Data Check: The error ratio histogram presented in Figure 8 includes two sets of field investigations. The major set, 31 comparisons, comes from the WES potomology studies of the Miss. R. bank sands with D_{50} from 0.12-0.27mm (Shockley & Strohm, 1961). Thirteen additional comparisons come from Florida Pamlico sands, mostly above the water table.

Of course, the collection of the Fig. 8 data include many possibilities for error other than in the Fig. 1 q_c-D_r correlation itself -- sampling disturbances; different methods for determining max and min D_r densities; possible sand cementation insitu; possible insitu overconsolidation; the use of mechanical cone tips; etc. Nevertheless, the histogram also suggests a normal distribution of error ratio when using Fig. 1, with a std. deviation of about 15%.

4.4 Overall: Considering all factors, and when using CPT data from electric, cylindrical tips in sands believed approximately similar to those used in the various UF chamber studies (NC, primarily quartz, recent, clean (no clay, less than 5% -200 sieve), below water table) the writer expects a std. deviation in D_r ratio of about 10-15%. Any single test point comparison could have an error of 35%.

Any further correction of q_c data obtained insitu for factors such as OC, using mechanical tips, geologically old and/or cemented sands, different sand grain mineralogy and/or size distribution, and partial saturation will likely increase the average D_r prediction error.

In connection with overall prediction accuracy, it may interest the reader to see how the updated correlation herein fits with other correlations collected by Mitchell and Gardner (1975, Fig. 30). Figure 9 presents this fit, showing general agreement with Thomas and with Turnbull et. al..

5. CORRECTIONS FOR OTHER FACTORS

5.1 Overconsolidation: Many chamber tests involving single cycles of K_o overconsolidation, to OCRs = 12, have demonstrated its great importance to any D_r evaluation from q_c. See Schmertmann (1972, 1974) and Veismanis (1974). OC greatly increases q_c, with all other variables

including D_r constant. To use Fig. 1 for OC sands the investigator must first correct the q_c data to reach the equivalent NC q_c. The writer suggests the following empirical formulas from Schmertmann (1975, p.84):

$$K_o'/K_o'_{NC} = (OCR)^{0.42} \quad \ldots\ldots\ldots\ldots\ldots (3)$$

$$q_c/q_{cNC} = 1 + 0.75\,((K_o'/K_o'_{NC}) - 1) \quad \ldots\ldots\ldots (4)$$

Using these formulas introduces further error, not only because of their approximate accuracy, but also due to the error when estimating the insitu OCR or the insitu K_o'. Note that roller compaction will also increase K_o'.

5.2 Delft Mechanical Cone Tips: As noted in section 3.1, Dr. Tumay's analyses of variances showed that the type of tip used (Fugro, advanced continuously, vs. Delft mechanical, advanced incrementally) as one of the least important variables. However, these analyses included mostly tests using air-dry, uniform, medium sands, with the UF chamber constant-stress boundary condition. The available comparisons from the field appear to show a distinct trend of difference in q_c with type of tip, depending primarily on the magnitude of q_c. Figure 10 presents these data.

Heijnen (1973), Joustra (1974) and Kok (1974) presented probably the currently most thorough field data, with subsequent statistical evaluations, comparing Delft and Fugro cone tip q_c's -- but all done at sites in The Netherlands. Their results illustrate the general uncertainty about the effects of tip shape and operation on q_c. Heijnen and Kok both found the Delft mechanical q_c significantly less than the Fugro electrical q_c, while Joustra found them about equal. The writer put in a trend curve in Fig. 10 as his estimate of the average best way to convert from $q_{c,mech}$ to $q_{c,Fugro}$ before entering Fig. 1.

5.3 Aging and Cementation: Geologically old sands and cemented sands will produce q_c data higher than if young and uncemented, at the same D_r. The writer knows of no quantitative data on this subject. We maintained chamber consolidation pressures for about 1 hr prior to cone tip insertion. The investigator can either just guess at a quantitative correction to his q_c before entering Fig. 1, ignore the correction and assume the sand will likely behave anyway as if it had the higher D_r predicted by Fig. 1, or by local site correlations change Fig. 1 to suit.

5.4 Medium and Coarse, Clean Sands: The available chamber tests suggest that a given q_c in such sands means a greater D_r than predicted from Fig. 1. As an approximation, increase D_r from Fig. 1 by a factor of 1.15. Do not use Fig. 1 for very coarse sands and gravel.

5.5 Fine, Silty Sands: All the sands investigated for this updated correlation had less than 5% passing the 200 sieve, and with no clayey fines. If your sand has clayey fines, or a significant % -200 (say 12% or more), relative density may represent a poor behavior-indicator parameter. For such sands use Fig. 1 cautiously. The presence of this much silt reduces permeability (probably to below 10^{-4} cm/s) and allows greater pore pressure generation, both + and -. As a result SM sands yield a lower q_c if loose, and a higher q_c if dense, than indicated by Fig. 1. Again, we lack quantitative data on this point and one must use judgement and possibly local correlation.

5.6 Well Graded Sands: The UF sand raining equipment can only prepare chamber samples using uniform sands with a low % -200. We have no tests on well graded sands. Some data presented by Muhs (1965) suggests that as a sand becomes more well graded its q_c reduces for a given D_r. Again, one must use judgement and possibly local correlation.

5.7 Above GWT, Partial Saturation: Because of capillary-induced negative pore water pressures, partially saturated sands found above the GWT have a higher effective stress state than computed from a simple overburden summation. They will therefore have a higher q_c and produce a too-high D_r when using Fig. 1 -- if all else equal. Plantema (1957) has presented some early chamber test data concerning the influence of partial saturation on q_c. The writer's experience in Florida suggests that this factor has only a minor influence. But, one must again use judgement and possibly local correlation.

6. REFERENCES CITED

Burmister, D. (1948), "The importance and practical use of relative density in soil mechanics," Proc. of the ASTM, Vol. 84, p.1

Caillemer, B. (1975), "An experimental study in the UF static cone test calibration chamber; Part I - Density distribution of pluvially placed sand," masters thesis to Dept. of Civil Engrg.

Heijnen, W. (1973), "The Dutch cone test; Study of the Shape of the electrical cone," 8th ICSM&FE, Vol. 1.1, pp. 181-184.

Harman, D. (1976), "Statistical study of static cone bearing capacity, vertical effective stress, and relative density of dry and saturated fine sands in a large triaxial test chamber," masters thesis to Dept. of Civil Engineering, August.

Joustra, K. (1974), "Comparative measurements on the influence of the cone shape on results of soundings," Proc. Stockholm ESOPT*, Vol. 2.2, p. 199. *European Symposium on Penetr. Testing

Kok, L. (1974), "The effect of the penetration speed and the cone shape on the Dutch static cone penetration test results," Proc. Stockholm ESOPT, Vol. 2.2, p. 215.

Laier, J., J. Schmertmann and J. Schaub, (1975), "Effect of finite pressuremeter length in dry sand,", ASCE, Specialty Conf. on Insitu Meas. of Soil Properties (SC-IMSP), Vol. 1, pp. 241-259.

Mitchell, J. and W. Gardner (1975), "In situ measurement of volume change characteristics," SOA paper to SC-IMSP, Vol. II, p. 279.

Muhs, H. (1965) Discussion in 6th ICSM&FE, Vol. III, p. 505.

Plantema, G. (1957), "Influence of density on sounding results in dry, moist and saturated sands," Proc. 4th ICSM&FE, Vol. I, p. 237.

Schmertmann, J. (1972), "Effects of insitu lateral stress on friction-cone penetrometer data in sands," Fugro Sondeer Symposium, pp. 37-39 (published by Fugro-Cesco, Holland).

Schmertmann, J. (1974), "Penetration pore pressure effects on quasi-static cone bearing, q_c," Proc. ESOPT, Vol. 2.2, p. 245.

Schmertmann, J. (1975), "Measurement of insitu shear strength," ASCE, SC-IMSP, Vol. II, p. 57 (SOA paper).

Shockley, W. and W. Strohm (1961), "Investigations with rotary cone penetrometer," Proc. 5th ICSM&FE, Vol. I, pp. 523-26. For more detailed data see "Rotary cone penetrometer investigations," U.S. Army Corps of Engineers, Waterways Experiment Station, Potamology Investigations, Report 18-1, June, 1962.

Veismanis, A. (1974), "Laboratory investigation of electrical friction-cone penetrometers in sand," Proc. Stockholm ESOPT, Vol. 2.2, pp. 407-419.

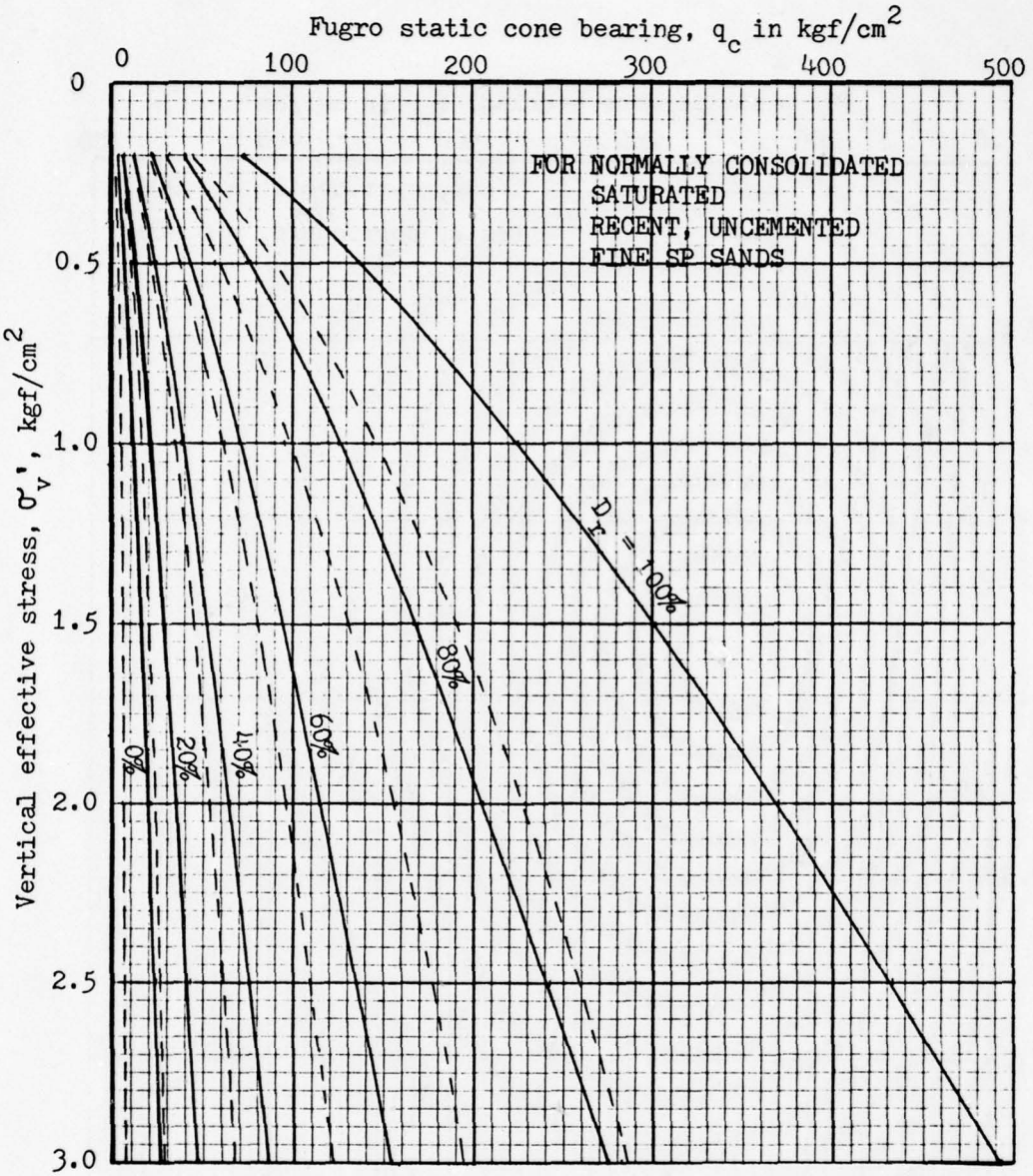

FIGURE 1 - UPDATED q_c-D_r CORRELATION (solid)
Previous correlation (dashed)

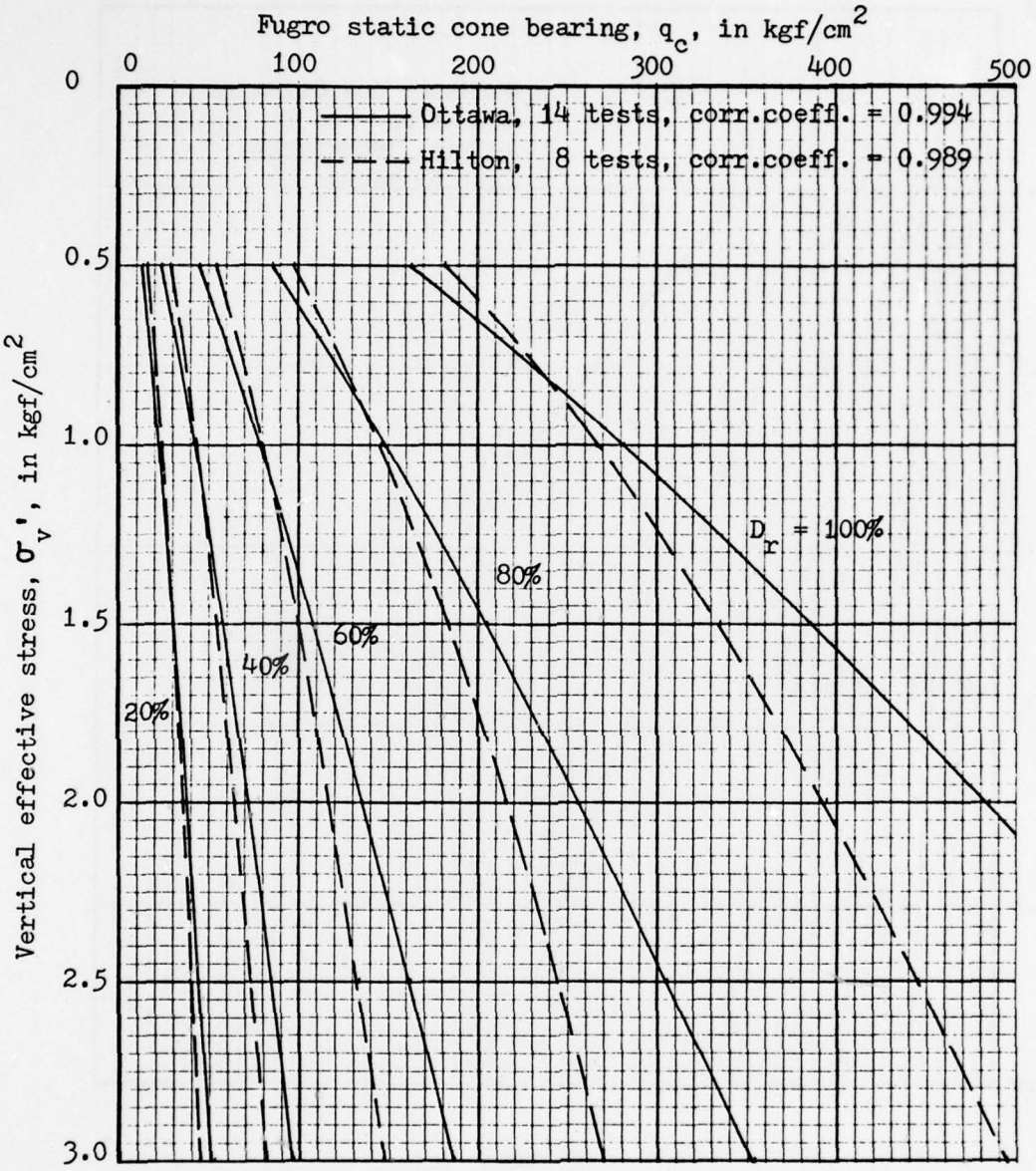

FIGURE 2 - COMPARISON OF REGRESSION ANALYSIS CURVES FOR THE DRY OTTAWA 90 AND HILTON MINES SANDS AT THE CONSTANT-STRESS BOUNDARY CONDITION

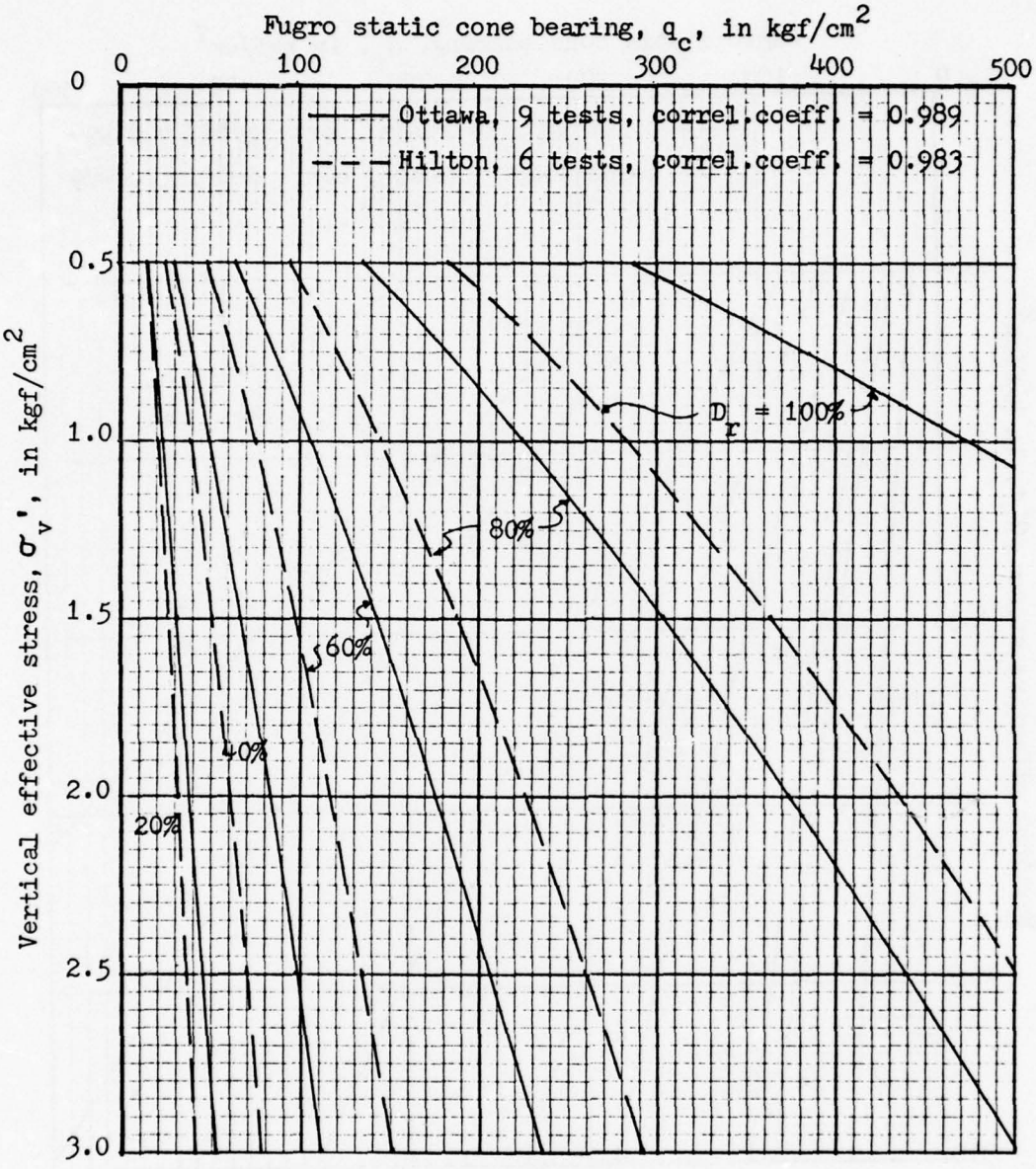

FIGURE 3 - COMPARISON OF REGRESSION ANALYSIS CURVES FOR THE DRY OTTAWA 90 AND HILTON MINES SANDS AT THE CONSTANT-VOLUME BOUNDARY CONDITION

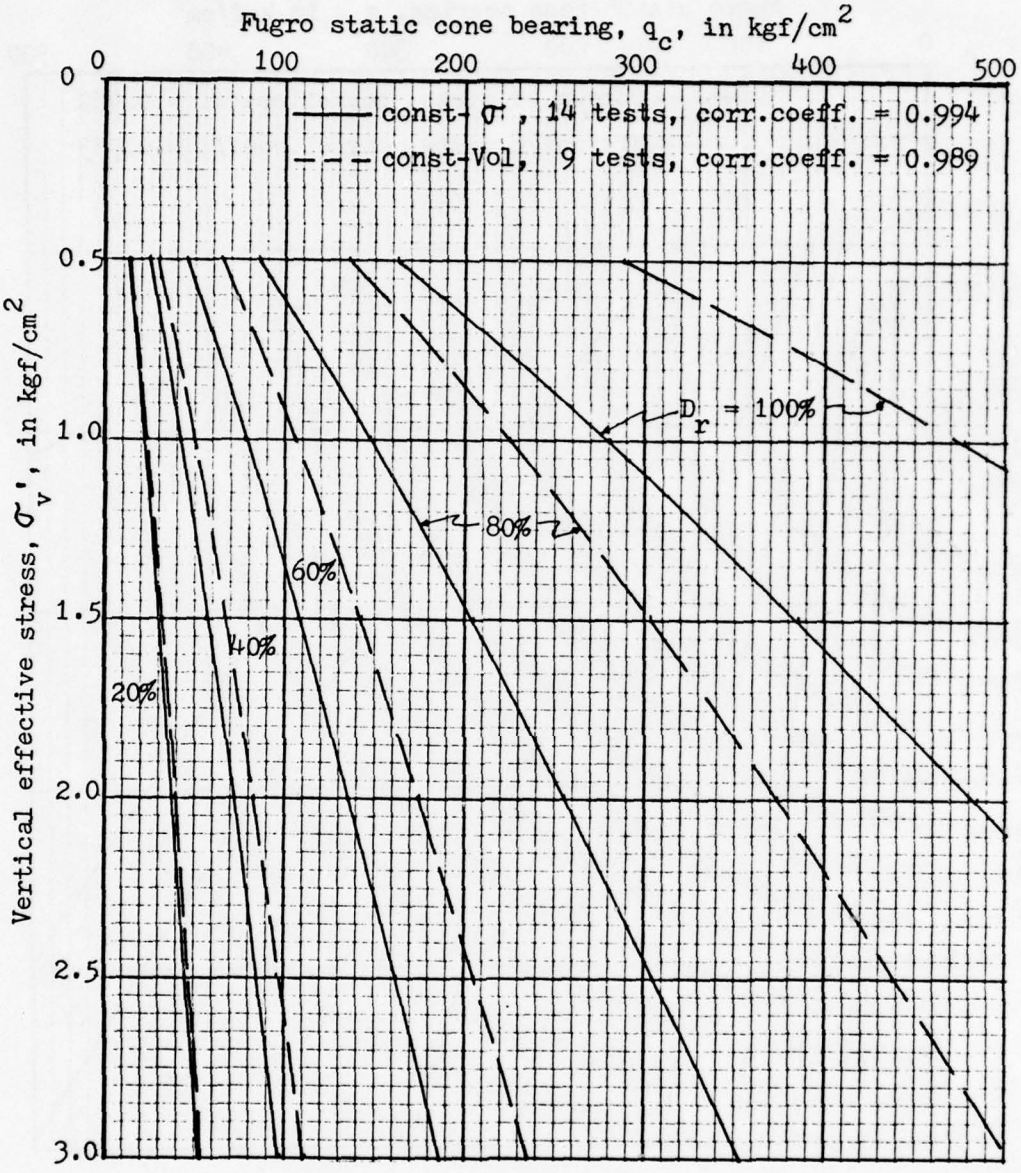

FIGURE 4 - COMPARISON OF REGRESSION ANALYSIS CURVES FOR THE DRY OTTAWA 90 UNCRUSHABLE SAND AT THE TWO BOUNDARY CONDITIONS

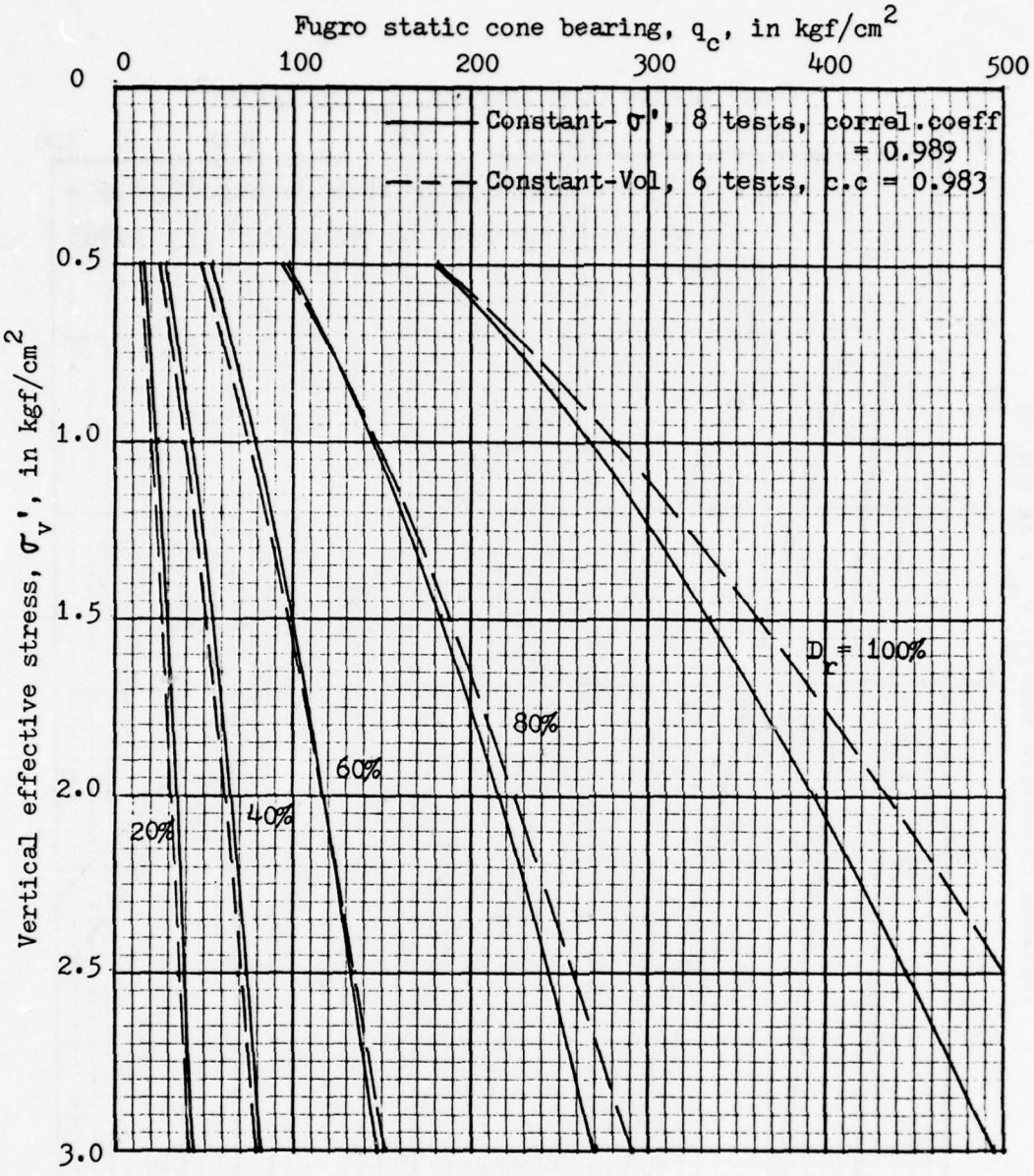

FIGURE 5 - COMPARISON OF REGRESSION ANALYSIS CURVES FOR DRY HILTON MINES CRUSHABLE SAND AT THE TWO BOUNDARY CONDITIONS

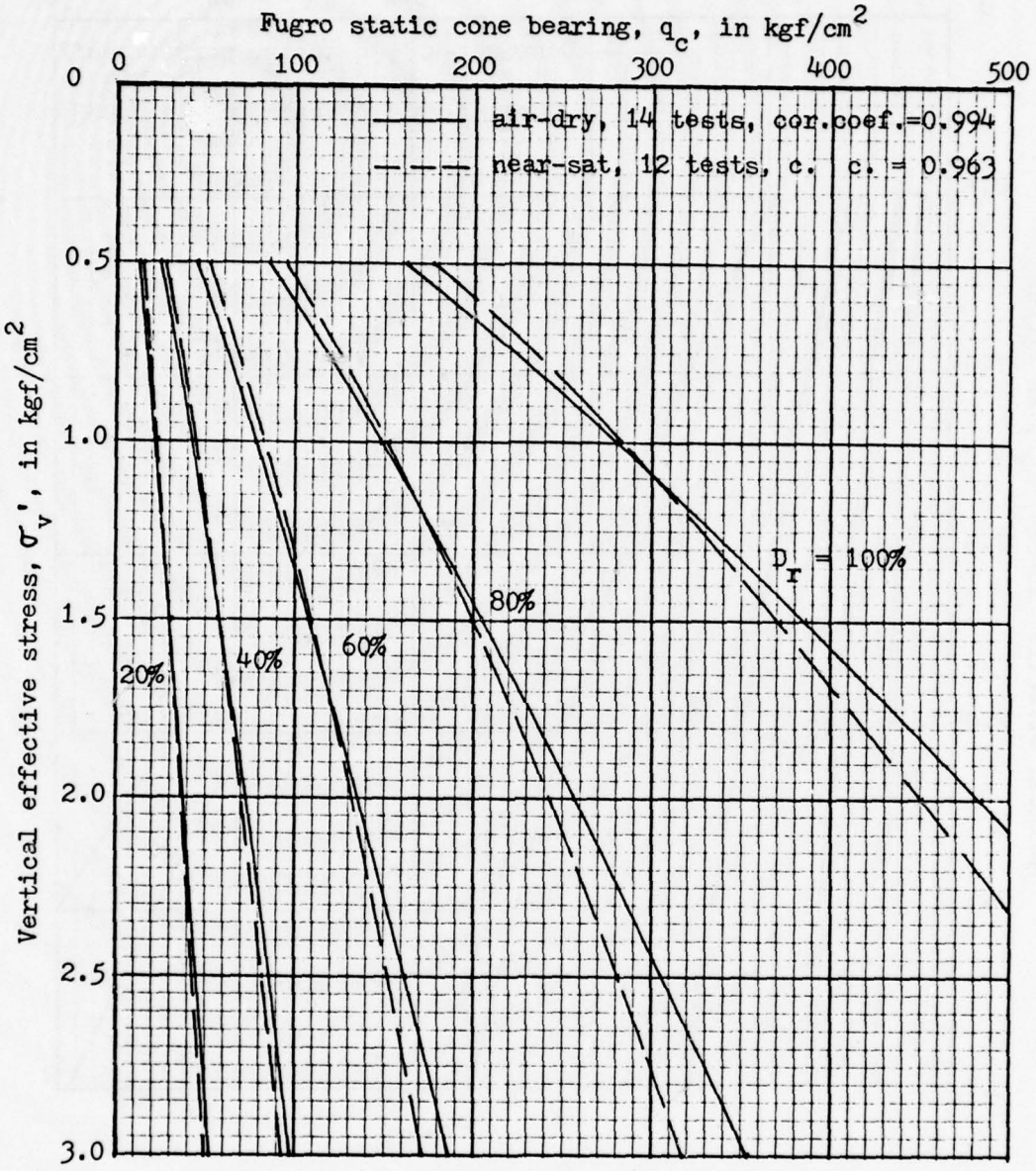

FIG. 6 - COMPARISON OF REGRESSION ANALYSIS CURVES FOR THE AIR-DRY AND NEAR-SATURATED OTTAWA 90 SAND

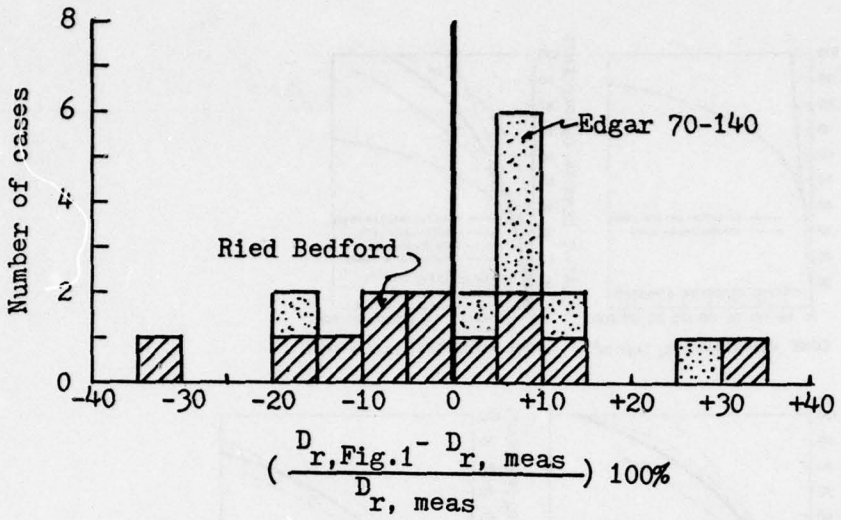

FIGURE 7 - HISTOGRAMS OF D_r ERROR RATIO USING FIG. 1 AND RESULTS OF ADDITIONAL CHAMBER TESTS USING EDGAR 70-140 & RIED BEDFORD SANDS

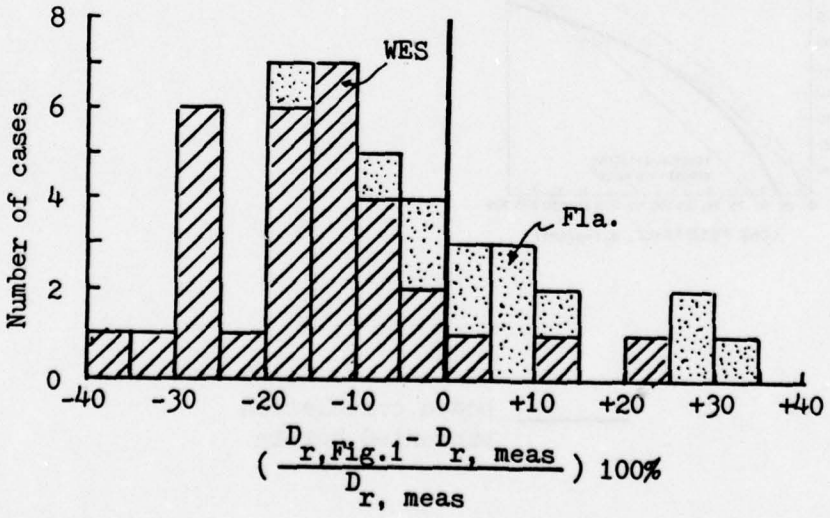

FIGURE 8 - HISTOGRAMS OF D_r ERROR RATIO USING FIG. 1 AND RESULTS FROM WES AND FLA. FIELD DATA

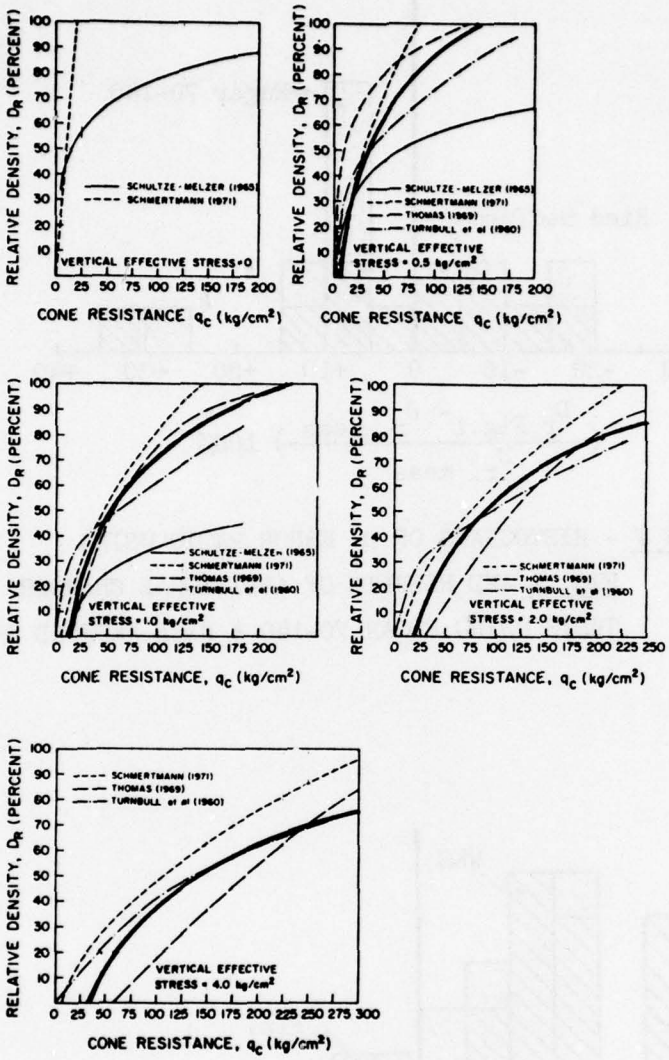

_____ added correlation
presented herein

FIGURE 9 - UPDATED q_c-D_r CORRELATION COMPARED WITH OTHERS COLLECTED BY MITCHELL & GARDNER (1975)

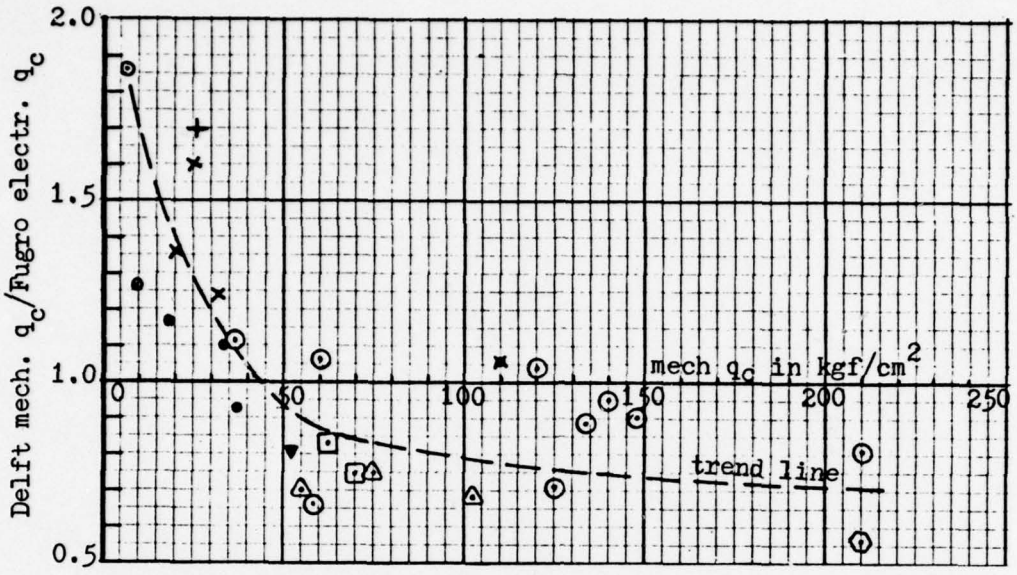

Legend:
- ⊙ Fugro tests, below WT (Joustra, 1974)
- ⊡ Delft tests, " " (Heijnen, 1973)
- △ Kok (1974), " "
- ⬡ U.F., field, " "
- + U.F., field, " " , sandy clay
- • U.F., field, above WT
- ▼ U.F., chamber, dry uniform med. sand
- ⊙ Ft. Pierce, Fla., silty sand below WT
- × Raleigh, NC, above WT, residual silt
- ✖ " " below WT, " "

All points represent averages of a layer at least 1.0m thickness.

FIGURE 10 - COMPARISONS BETWEEN q_c OBTAINED WITH DELFT MECHANICAL AND FUGRO ELECTRIC STATIC CONE TIPS

PHASE II - LABORATORY STUDY

9. INTRODUCTION

I continued the investigation of the feasibility of using the Wissa type piezometer probe to identify the liquefaction potential of saturated, fine sands by performing special probe soundings in the University of Florida laboratory calibration chamber. Please add this Phase II part of the report directly to the previous Phase I report of 8 Oct 76 to form the final, total report. All figure, table, appendix and report section numbers herein continue the numbering sequence begun in the Phase I report.

9.1 Purpose of Phase II

In the Phase I field tests we had natural insitu boundary conditions and a probable natural degree of saturation at or very near 100%. But, in the field we do not know accurately the insitu stresses nor the sand's dry unit weight or relative density.

In contrast, in the laboratory we can know the stresses and densities accurately. But, the boundary conditions and degrees of saturation achieved probably match only crudely the ordinary field situation. Each pilot study location thus offers its advantages and disadvantages. We hoped for maximum information by performing piezometer probe soundings both in the field and in the laboratory.

9.2 Scope of Phase II

The scope of the laboratory work consisted of four probe soundings, one each in four separate fillings of the special University of Florida test calibration chamber. We tested the Reid Bedford Model sand (RBMS) supplied some time ago by WES for other purposes. Because of the effects of our sand raining and drying operations we have lost most of the -200 sieve fines from this sand. A recent check shows we now have about 1% -200.

For three of the chamber tests we used the same Wissa probe as we used in Phase I. At the time of testing these tests had the sand at relative densities of 32%, 61% and 81%, and a whole-chamber average degree of saturation of 97%. The remaining chamber test used the same UF probe

used in Phase I, with 30% relative density and 97% saturation.

In all Phase II tests we kept the sand in an approximately normally consolidated state with a mid-height vertical effective stress of $17\frac{1}{2}$ psi and $K_o' = 0.46$.

10. DESCRIPTION AND USE OF THE UF CALIBRATION TEST CHAMBER

10.1 General

The UF chamber used for this study contains a 4.0 ft diameter, 4.0 ft high sample of sand. Rubber membranes and water surround the sample vertical cylindrical perimeter and horizontal bottom. The top of the sand makes contact with a relatively rigid, micarta platen with a 2.4 in. diameter access hole at its center. This hole permits the axial insertion of any suitable type of test instrument, such as the piezometer probes used in this study.

Figure 10 presents a series of photos which shows the chamber at various stages during sample preparation and testing. Figure 11 shows a cross-section of the chamber, including the support system of tanks, valves, etc.

The following explains the various test operations in more detail.

10.2 Sand Filling

Before any sand filling, the side rubber membrane is held evenly against a cylindrical sheet metal sample former by means of vacuum pressure. Then we place the special copper tubing CO_2 and water diffuser system, shown in Fig. 10(a), on the bottom membrane in the empty chamber. Sand, previously dried by a hot-air blower system, is then placed into the overhead hopper shown in Fig. 10(b). This hopper travels back and forth at a constant elevation on a rail system spanning the top of the sample chamber. The sand leaves the hopper when the operator opens a set of scissor-acting shutter plates to match the sets of holes in these plates. The sand then falls thru these plates on to and thru a series of wire screens designed to provide a uniform raining intensity thru the bottom screen.

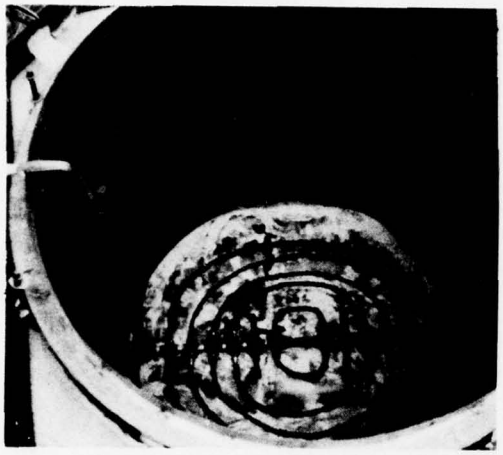

(a) Empty chamber showing bottom & side rubber membranes with porous copper tubing grid at bottom used to move CO_2 and water up thru sand

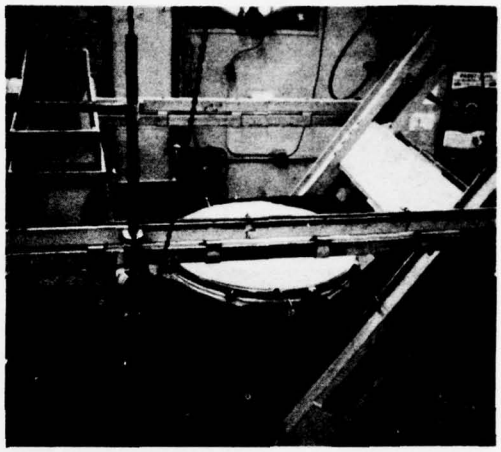

(b) Chamber filled with dry sand by raining from hopper (left) moving back & forth on rails; load frame tilts out of way

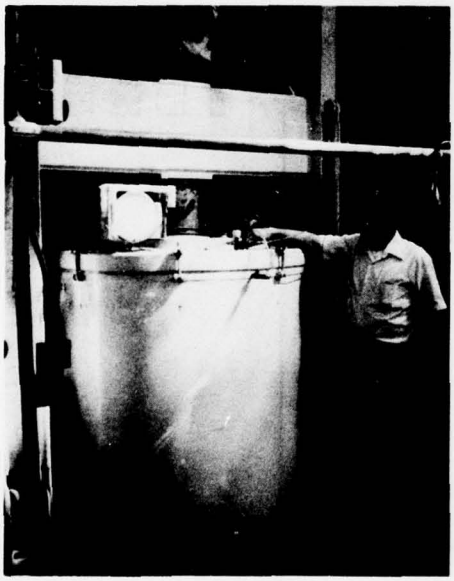

(c) Chamber sealed and pressurized, sand saturated, load frame tilted back to vertical for test, probe ready for axial insertion

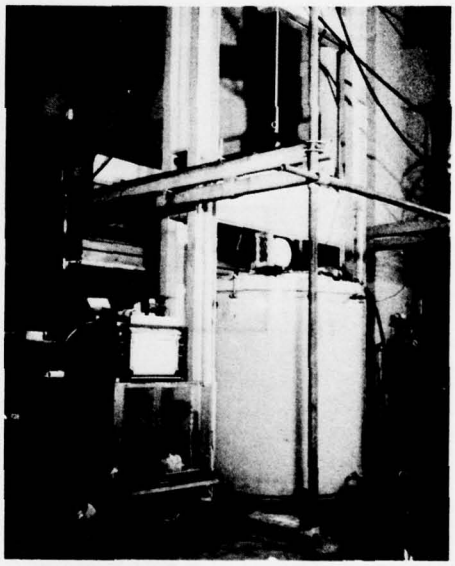

(d) Entire chamber setup ready for test; hydraulic piston pushes probe at constant rate, chart recorder plots probe transducer data continuously

FIGURE 10 - UNIVERSITY OF FLORIDA K CONSOLIDATION, 4 FT HIGH, 4 FT DIAM., TRIAXIAL SAND CHAMBER

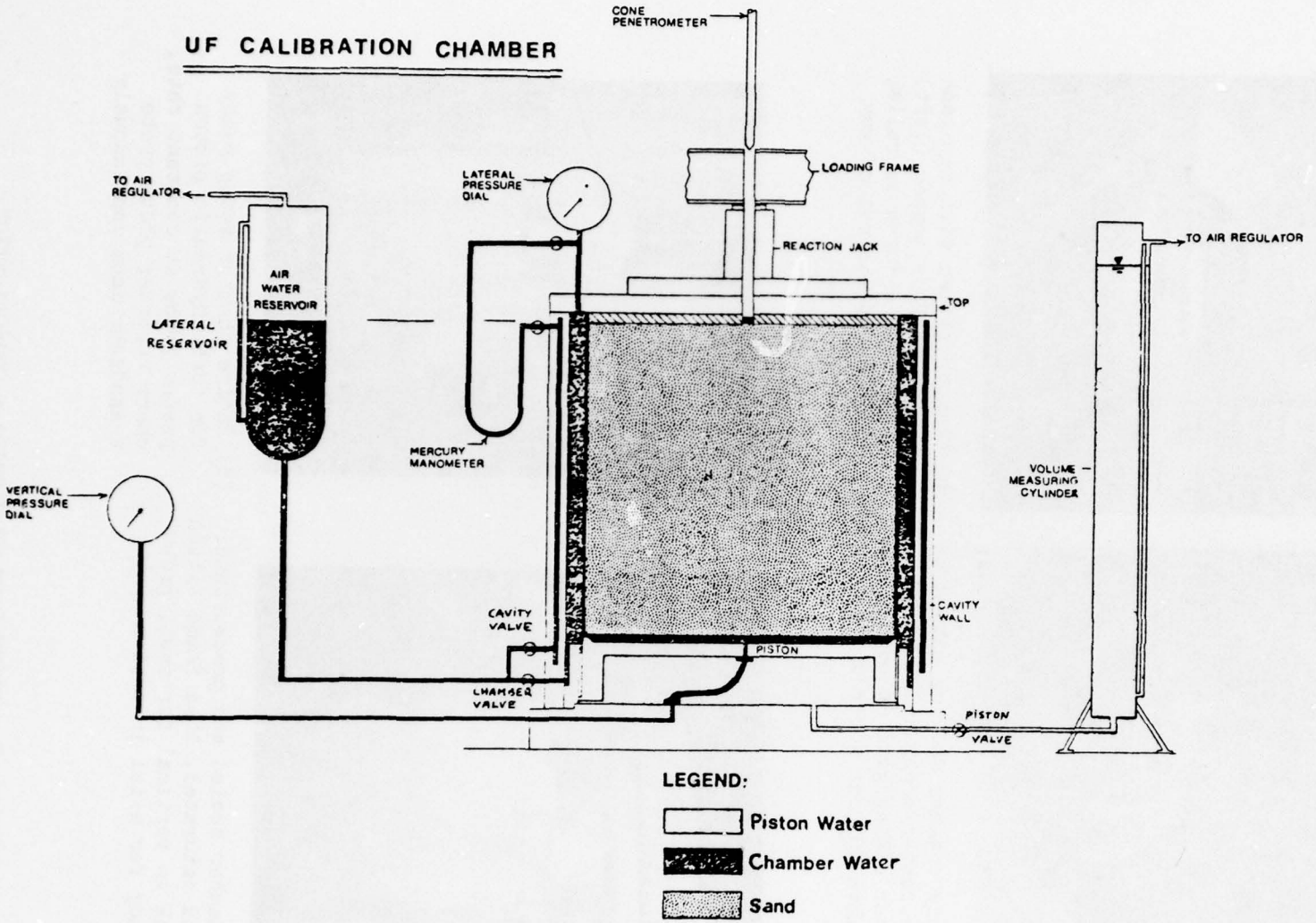

FIGURE 11 - Principal Features of the UF Calibration Chamber

We achieve different sample relative densities by using shutter plates with different hole diameters and spacings. The larger the holes, and at the same time the greater the percent of the plate area taken by these holes, the greater the raining intensity (lbs/min) and the lower the resulting relative density. For this research we used shutter plates with 3/16, 3/8 and 5/8 inch diameter holes, covering 1.0%, 4.2% and 11.6% of the plate areas, respectively.

The constant elevation of the hopper and bottom screen below the hopper results in a variable height of sand drop as the chamber fills with sand -- varying from 4.9 ft when empty to 0.9 ft when full. Careful investigation has shown that the sand fills the chamber with an approximately random dry density variation of $\pm 1\frac{1}{2}$ pcf. Such variation probably also occurs in natural sand deposits that we might ordinarily consider of uniform density. Also, many cone penetration tests of different types in the chamber have shown, by the uniformity of the data produced, that we achieve essentially uniform dry density conditions in this chamber with the method of deposition just described.

10.3 Saturation and Pressure Application

After raining in the sand on top of the diffuser system shown in Fig. 10(a), the sand fills the chamber as shown in Fig. 10(c). We then pass CO_2 gas thru the diffuser system and upward thru the sample to flush out the air between the sand grains and replace it with CO_2. For this purpose we use a volume of CO_2 about 10 times the volume of voids in the sand sample.

Following the air replacement by CO_2 we allow water to slowly enter the sand by upward flow thru the diffuser system. We do this very slowly, taking about 15 hours to complete the saturation. But, before starting this water flow we place the lids on the chamber and pressurize the sand sample to a bottom vertical effective stress of 10.0 psi, using K_o consolidation. This prevents the quicksand action that would otherwise occur during upward water flow.

We have the water tank elevation adjusted such that the head causing the flow reduces to zero when the chamber just fills with water. This

tank rests on a lever system that includes a force transducer. By monitoring this transducer we can measure the weight of water that flows into the chamber sand, 1125 to 1300 lbs in the Phase II tests, to ± 2 lb. This permits us to measure the degree of saturation achieved for the entire sand sample to a precision of about ± 0.2%.

Following the shut off of the water flow we subjected the now near-saturated sand sample to a further K_o consolidation by increasing the air pressure acting on the bottom piston. During this increase we adjusted the lateral (radial) pressure to keep the average volume change along the vertical sides of the cylindrical sample at zero by means of a differential mercury manometer null system. In all tests for Phase II we increased the total pressure at the bottom piston to 20.0 psi. This produced an effective vertical stress at specimen mid-height of about 17.5 psi. The K_o consolidation produced an effective horizontal stress of about 8.0 psi at specimen mid-height, for a $K_o' = 0.46$. By these methods we produced an approximately normally consolidated sand sample prior to inserting the piezometer probe.

10.4 The Piezometer Probe Soundings

Just as described for the Phase I field tests, we first saturated the probe tips, assembled them under water, placed a bag of water with a sponge around the tip and taped the system together so as to maintain tip saturation during the other preparations for probe insertion into the chamber sample. We then lowered the bagged tip to the free water standing an inch or so above the top of the sand in the axial access hole. The probe insertion broke the bag. This insertion involved a single stroke at 2 cm/s with a hydraulic jack controlled to provide a constant rate of penetration. During this insertion we kept both total vertical and radial sample boundary stresses constant at the same value they had after K_o consolidation, but allowed the boundary volumes to change. As in Phase I, we made a continuous chart record of the pore pressure response of the penetrating probe during its 1.0 meter penetration into the chamber sample, using the same signal conditioning and recording equipment used in Phase I.

11. TEST SERIES PERFORMED

As noted previously, the Phase II tests consisted of four separate piezometer probe chamber tests, three using the Wissa probe and one the UF probe. Table 3 summarizes the test conditions with respect to pressures, relative density and percent saturation. This table also includes the probable CPT q_c value that we would have obtained had we tested these chamber samples with the Delft mechanical mantle cone tip used in the Phase I field work. These q_c estimates have their bases in previous constant-stress boundary condition chamber tests on near-saturated Reid Bedford Model Sand, as noted on p. 3 of Appendix III. These q_cs also include a correction for the use of the Delft mechanical cone tip, as noted in Fig. 10 of Appendix III.

Table 3 - TEST CONDITIONS

Test No.	Date	Probe	Plate holes	Mid-ht pressure σ_v'	σ_h' (psi)	γ_d* (pcf)	D_r (%)	S (%)	Delft q_c (ksc)
1	21 Sep	W	3/16"	17.40	7.85	103.1	81	96½	105
2	27 Sep	W	5/8"	17.50	7.91	93.95	32	97	38
3	1 Oct	UF	5/8"	17.50	8.20	93.5	30	97	36
4	7 Oct	W	3/8"	17.44	8.10	99.1	61	97	67
added test 5	15 Nov	UF	5/8"	17.5	8.24	93.7	31	97	37

*After-consolidation condition, estimated from before-consolidation condition from previous testing. Effects calculations for D_r, S and q_c.

We also performed 3 separate fillings of the chamber only for the purpose of adding to our previous data base for estimating the dry density and relative density at which the sand filled the chamber from the raining deposition described in 10.2. We did not saturate after these fillings but only removed and weighed the sand to get an accurate measurement of its deposited, whole-chamber-average unit weight. For practical reasons we cannot weigh the sand following saturated tests and must base our density estimates on previous fillings with the same sand and shutter plates when using dry sand. We have learned from experience that we can reproduce relative densities with a std. deviation of about 1 part in 20 (2½% @ 50%).

11.1 Excess Hydrostatic Pore Pressures

I reduced the continuous chart records of tip pore pressure vs. time during the 1.0 m penetration of the chamber sample during each test to extract the depth variation of excess hydrostatic pore pressure. I defined this as the difference between measured pore pressure and that equilibrium pore pressure measured at the end of the 1.0 m of probe penetration, proportioned to the depth considered in relation to 1.0 m. Table 4 lists the results:

Table 4 - SUMMARY OF CHAMBER TEST RESULTS

Test No.	1	2	3	4	added 15 Nov. 5
Probe used	Wissa	Wissa	UF	Wissa	UF
Ave. rate penetr (cm/s)	2.07	2.07	2.05	2.10	2.30
excess equilibrium pore water pressure 10 cm		0.25psi	0.1psi	0.1psi	
20	-0.25psi	0.15	0.3	-.2	
30	-.3	0.1	0.4	-.25	0.25
40	-.35	0.0	0.35	-.2	0.29
50	-.35	-.05	0.2	-.25	0.31
60	-.4	-.05	0.05	-.3	0.31
70	-.45	-.05	-.15	-.35	0.34
80	-.45	-.05	-.25	-.45	0.42
90	-.5	0.0	-.45	-.5	
100	-.55	0.0	-.55	-.5	0.54
Equil pp (psi)	0.95	1.30	0.85	1.00	1.39
vs. hydr.@ 1 m	1.42	1.42	1.42	1.42	1.42
Probe sensitiv. checks in water bucket: Before:	--	OK	½ sens.	OK	OK (special care) OK
After test :	OK	OK	½ sens.	--	

We set the chart recorder at a sensitivity of 1 div = 1.0 psi for both probes, with 0.2 inches/div, and ran the chart at a speed of 4 inches/min during the 0.8 min required for the 1 meter penetration. We checked the probe calibrations before test 1 and after test 4 and found them the same. We also checked probe sensitivity by moving the probe up and down about 9 inches in a water bucket before and/or after each test, as noted in Table 4. With the exception of only about ½ response with the UF probe in this bucket test, we found the system recording with the proper sensitivity in all checks. A subsequent check of the UF probe calibration showed it OK. We did not consider the UF probe test results different enough to repeat for this report.

11.2 Sand Permeabilities

To provide associated data of importance in evaluating the results of this pilot study, we performed laboratory permeability tests on both the Phase I tailings sand and the present Phase II Reid Bedford Model sand. Figure 12 presents the results from our tests, for both sands, showing how we found permeability to vary with each sand's relative density.

With the tailings sand we used only small sample (62 cm^3, miniature compaction mold), high gradient, constant head tests. With the RBMS we used primarily the entire chamber sample and measured the flow of water from the bottom diffuser when maintaining a head difference of only a few inches over the 4 ft sample height. A single small sample test on RBMS gave results that matched the chamber tests.

11.3 Compressibility of RBMS

Because pore pressures around a penetrating object depend not only on permeability, but also on soil compressibility, we also measured the compressibility of the RBMS during the K_o consolidation in the test chamber. The following Table 5 summarizes our findings, expressed in terms of volume strain per change in octahedral effective stress. Although we found a somewhat non-linear behavior over the 5 to 25 psi octahedral stress range investigated, the table presents a single, average value.

Table 5 - MEASURED 1-D COMPRESSIBILITY OF RBMS

D_r %	K_o	Compress. (ft^2/lb)
29	0.40	2.23×10^{-6}
	0.46	2.05
81	0.38	10.31×10^{-7}
	0.45	9.39

11.4 Grain Size Distribution of RBMS

Figure 13 presents the results of a representative, recent sieve analysis of the Reid Bedford Model Sand used in this Phase II study.

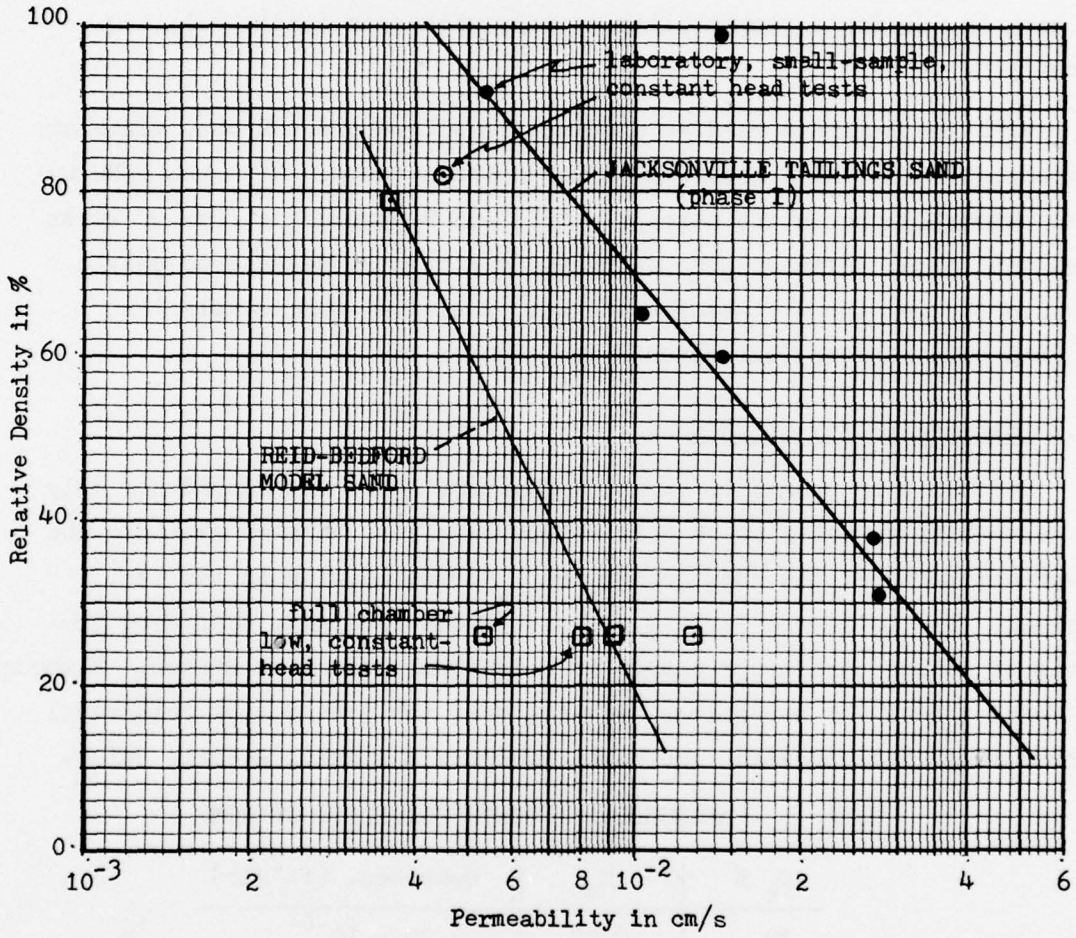

FIGURE 12 - RESULTS OF SMALL AND LARGE SAMPLE LABORATORY CONSTANT HEAD PERMEABILITY TESTS ON TAILINGS & REID BEDFORD SANDS

GRAIN SIZE DISTRIBUTION

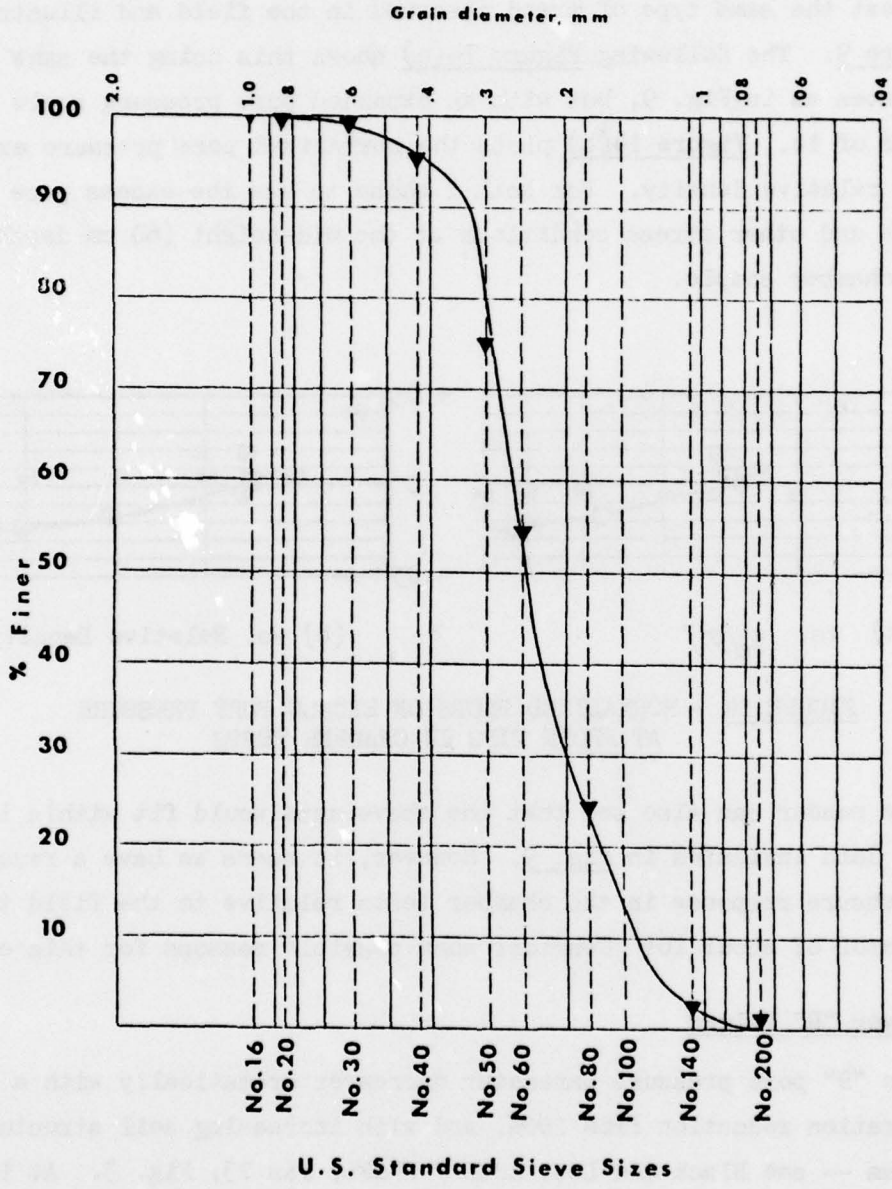

FIGURE 13 - SIEVE ANALYSIS OF REID BEDFORD MODEL SAND USED IN PHASE II STUDY

12. ANALYSIS OF PHASE II TEST RESULTS

The reader will see from Table 4 that each of the four chamber tests produced very little pore pressure response at the tip of the penetrating probes. But, despite their low magnitudes, these data do suggest the same type of trend observed in the field and illustrated by Figure 9. The following Figure 14(a) shows this using the same coordinates as in Fig. 9, but with an expanded pore pressure scale by a factor of 10. Figure 14(b) plots the normalized pore pressure excess against relative density. For both I chose to use the excess pore pressure and other stress conditions at the mid-height (60 cm depth) of the chamber sample.

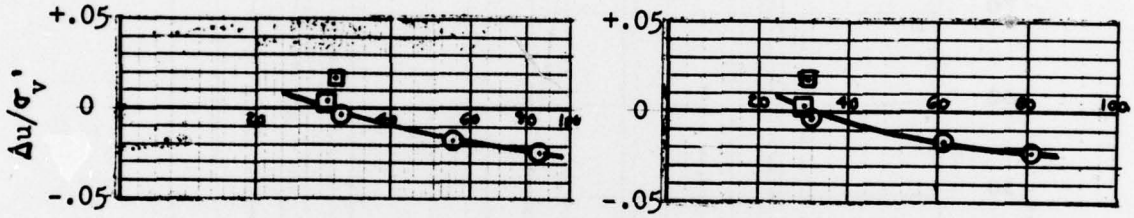

(a) vs. q_c/σ_v' (b) vs. Relative Density %

FIGURE 14 - NORMALIZED PLOTS OF EXCESS PORE PRESSURE AT PROBE TIPS IN CHAMBER TESTS

The reader can also see that the above data would fit within the band of data indicated in Fig. 9. However, it seems we have a reduced pore pressure response in the chamber tests relative to the field tests by a factor of about 10! Consider some possible reasons for this effect.

12.1 Lower "B" Values

The "B" pore pressure parameter decreases dramatically with a degree of saturation reduction from 100%, and with increasing soil structure stiffness -- see Black and Lee, ASCE J-SM&FD, Jan 73, Fig. 3. At 100% saturation "B" has a value of almost 1.00 for all ordinary soils. I assume a value of almost 1.00 applied to the insitu Phase I tailings sand. However, in sands with a degree of saturation of only 97%, as Table 3 indicates we had for the Phase II chamber tests, Black and Lee suggest

we might have "B" only about 0.1 in these tests.

If probe pore pressures result primarily from spherical stress change effects, or if the deviatoric "A" pore pressure parameter changes with partial saturation in a ratio similar to the "B" changes, then the lack of 100% saturation in the chamber test samples alone could explain the factor of 10 reduction in generated pore pressures.

12.2 Other Possible Reasons

Chamber boundary conditions: The fixed, no-flow, boundary of the chamber at a 2.0 ft radius from the probe insertion can affect pore pressure buildup at the probe. Preliminary studies suggest that this boundary effect may increase chamber pore pressures by a factor as great as 5 compared to the field, no-boundary, case.

On the other hand we also employed the constant-stress boundary condition, which allows more deformation of the soil mass than would the field situation. Preliminary studies suggest that decreasing sample rigidity would decrease pore pressures by a factor as much as 2.

Permeability differences: Figure 12 showed that the chamber sand may have had a permeability about 1/3 that of the sand in the field (RBMS vs. tailings). This would tend to increase chamber pore pressures by some unknown factor.

13. CONCLUSIONS FROM PHASE II

13.1 - The data obtained from the four lab chamber tests indicates the same general pattern of pore pressure response found in the Phase I field tests, but at magnitudes reduced by a factor of about 10.

13.2 - This factor of 10 most likely results from the difference between the 100% (assumed) saturation condition in the field and the S = 97% computed to exist during the chamber tests. We must achieve 100% saturation for viable lab tests to evaluate such probe behavior.

13.3 - These Phase II studies do not alter my previous general conclusions with respect to using piez. probe soundings for evaluating liquefaction potential in saturated, fine sands.

In accordance with letter from DAEN-RDC, DAEN-ASI dated 22 July 1977, Subject: Facsimile Catalog Cards for Laboratory Technical Publications, a facsimile catalog card in Library of Congress MARC format is reproduced below.

Schmertmann, John H
Study of feasibility of using Wissa-type piezometer probe to identify liquefaction potential of saturated fine sands / by John H. Schmertmann, University of Florida, Gainesville, Florida. Vicksburg, Miss. : U. S. Waterways Experiment Station ; Springfield, Va. : available from National Technical Information Service, 1978.
73 p. : ill. ; 27 cm. (Technical report - U. S. Army Engineer Waterways Experiment Station ; S-78-2)
Prepared for Office, Chief of Engineers, U. S. Army, Washington, D. C., under Contract No. DACW39-76-M-6646.
References cited: p. 50.

1. Cone penetrometers. 2. Fine grained soils. 3. Liquefaction (Soils). 4. Pore pressure measurement. 5. Relative density. 6. Sands. 7. Saturated soils. 8. Wissa-type piezometer probe. I. Florida. University, Gainesville. II. United States. Army. Corps of Engineers. III. Series: United States. Waterways Experiment Station, Vicksburg, Miss. Technical report ; S-78-2.
TA7.W34 no.S-78-2